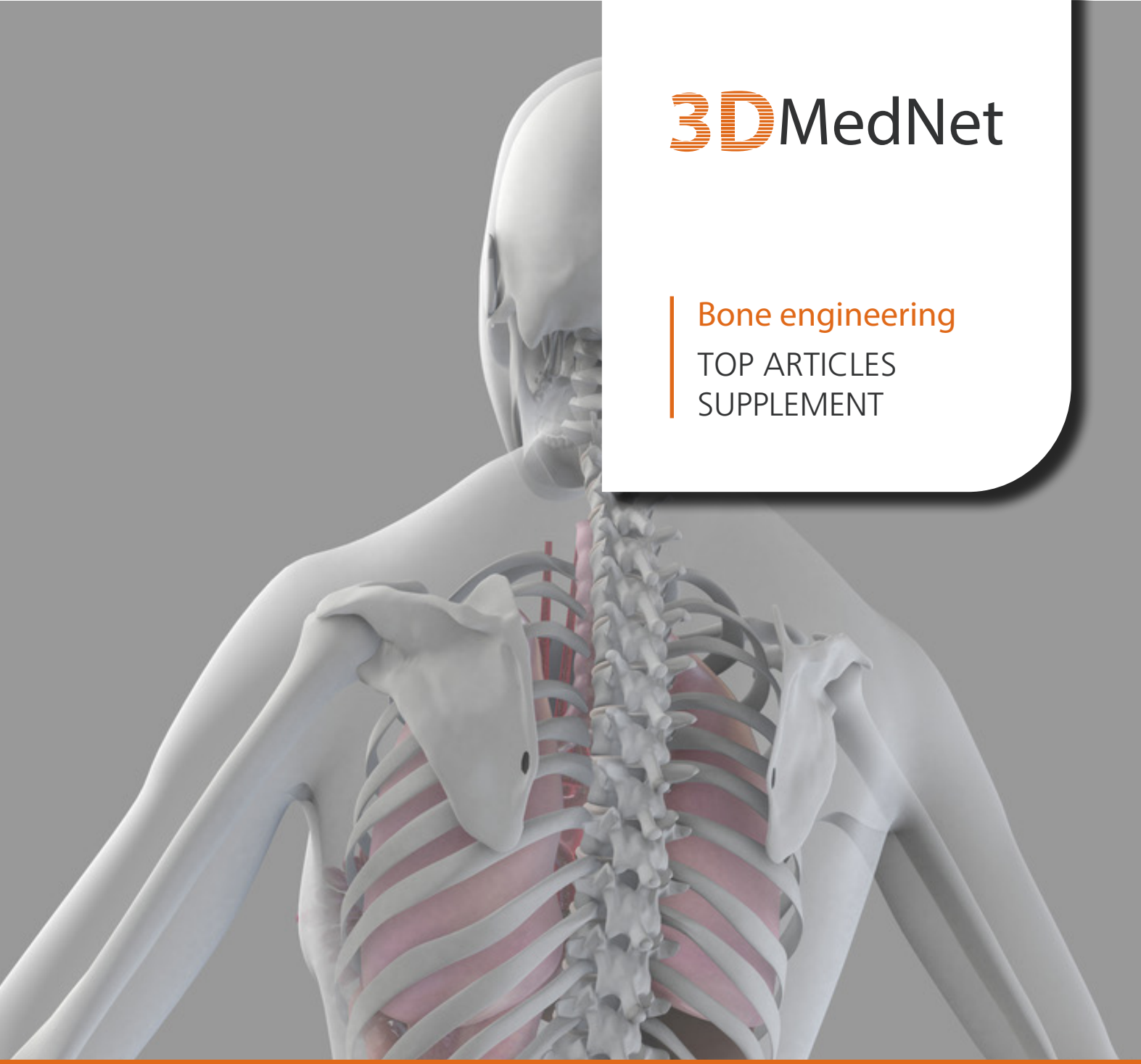

3DMedNet

Bone engineering

TOP ARTICLES SUPPLEMENT

CONTENTS

fsg CONNECT

Review

For reprint orders, please contact: reprints@futuremedicine.com

Regenerative Medicine

Hope versus hype: what can additive manufacturing realistically offer trauma and orthopedic surgery?

Additive manufacturing (AM) is a broad term encompassing 3D printing and several other varieties of material processing, which involve computer-directed layer-by-layer synthesis of materials. As the popularity of AM increases, so to do expectations of the medical therapies this process may offer. Clinical requirements and limitations of current treatment strategies in bone grafting, spinal arthrodesis, osteochondral injury and treatment of periprosthetic joint infection are discussed. The various approaches to AM are described, and the current state of clinical translation of AM across these orthopedic clinical scenarios is assessed. Finally, we attempt to distinguish between what AM may offer orthopedic surgery from the hype of what has been promised by AM.

Keywords: additive manufacturing • bone graft • orthopedic surgery • 3D printing

David MR Gibbs*[,1], Mohammad Vaezi[2], Shoufeng Yang[2] & Richard OC Oreffo[1]

[1]Bone & Joint Research Group, Centre for Human Development, Stem Cells & Regeneration, Institute of Developmental Sciences (MP887), Southampton General Hospital, University of Southampton, Southampton, Hampshire S016 6YD, UK

[2]Faculty of Engineering & the Environment, University of Southampton, Southampton, SO17 1BJ, UK

*Author for correspondence: dmg1e12@soton.ac.uk

The hype of additive manufacturing

Additive manufacturing (AM) has been used to produce everything from guns to models of unborn babies. In excess of 1450 articles pertaining to AM are listed in PubMed, around a third of which were published in the last 2 years alone. Attempts are being made to use AM to form human organs; indeed, some authors have commented that for hard tissue applications, the barriers for clinical translation are now regulatory rather than scientific or technical [1]. By contrast, other researchers believe that there are still a number of problems that must be solved before we can see the availability of scaffolds for clinical purposes [2].

Unmet clinical needs in trauma & orthopedic surgery

To understand the potential of AM in orthopedics, it is necessary to first evaluate the clinical need and current limitations to treatment. Areas to be addressed include bone defects, spinal arthrodesis, chondral injury and periprosthetic joint infection (Figure 1).

Bone graft material is frequently required to fill voids to enable a mechanically stable reconstruction in trauma and orthopedic surgery. Currently, in excess of 2 million grafting procedures are performed annually [3], with the material used either isolated from the patient (autograft), a donor (allograft) or the application of synthetic materials. Harvesting of autograft results in patient morbidity [4] and the amount available is finite. Furthermore, the use of allograft may result in disease transmission or an immunological reaction at the graft site. To date, 59 synthetic bone substitutes are available for clinical practice in the UK [5], while their composition varies, in the mainstay, the materials are limited by poor control of porosity and rate of degradation. Ideally, bone graft material should be: osteogenic (contain bone-forming cells), osteoconductive (permit migration of bone cells) and osteoinductive (stimulate osteogenic differentiation). Autograft remains the only material to retain any significant osteogenicity. Furthermore, none of these three categories of graft are vascularized, nor can the materials, including autograft, be readily formed/moulded to match the defect site.

Spinal arthrodesis is a common surgical procedure [6] used to treat pain and restore

Future Medicine part of fsg

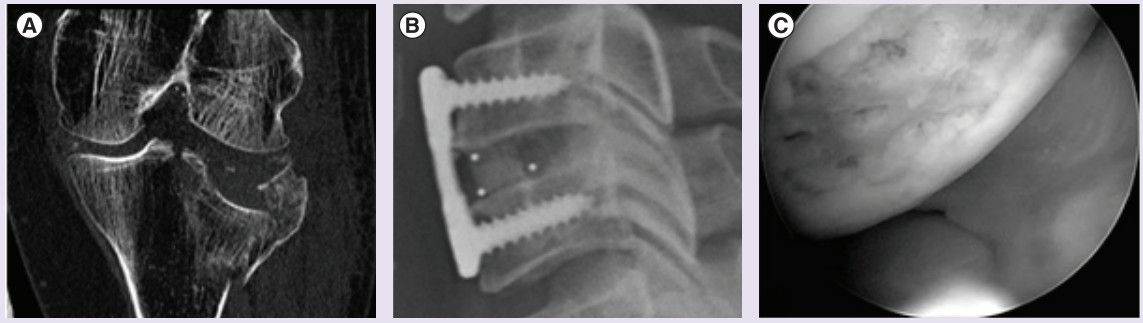

Figure 1. Clinical requirements in trauma and orthopedic surgery. (A) Tibial fracture requiring bone graft, **(B)** spinal cage device and **(C)** chondral defect post microfracture.

stability in a wide range of conditions including trauma, deformity and degenerative disease. Surgical techniques vary according to the disease, spinal location and patient and surgical factors [7]. In selected cases, cages may be used in combination with bone graft or an osteoinductive material to provide immediate mechanical support and to facilitate fusion. Devices are typically comprised of titanium or polyether ether ketone. However, disadvantages of using these permanent materials include subsidence and stress shielding [8].

Chondral injury, in other words damage to articular cartilage, is relatively common [9] and results in symptoms such as pain and loss of function for the patient. Current treatment strategies include microfracture and autologous chondrocyte implantation (ACI). Microfracture involves drilling through the lesion into the subchondral bone to stimulate the production of fibrocartilage from the underlying marrow. However, fibrocartilage remains biomechanically inferior to hyaline cartilage; this may explain the poorer long-term outcome in patients observed with this technique compared to ACI [10]. By contrast, ACI involves harvesting 'donor' chondrocytes from the patient's knee, *ex vivo* expansion, seeding of the expanded cells onto a scaffold and placement into the defect during a second surgical procedure. While ACI produces a superior long-term clinical outcome [10] compared with other treatment strategies, limitations include: requirement for 'donor' chondrocytes, subjecting the patient to two procedures, cell expansion and the formation of scaffold material to match the defect.

Periprosthetic joint infection is a devastating complication affecting between 1 and 3% of joint replacements. In addition to the human cost, given that in excess of 180,000 lower limb arthroplasties are performed annually in England and Wales [11], this represents a huge burden in terms of healthcare provision. The accepted gold standard treatment involves resection of implants and placement of an antibiotic-impregnated cement for a minimum of 6 weeks followed by reimplantation of the prosthesis [12]. While antibiotic-impregnated cement facilitates a prolonged release of antibiotics, cement may only be combined with antibiotics that are thermostable due to the exothermic nature of cement process and the high temperatures generated.

The focus of this article is on the current applications and limitations of AM for orthopedic translation. A number of AM reviews detailing the processes therein have recently been published [13,14,34]. Critically, the focus is on the identification of what the technology of AM may achieve, as opposed to the hype of what has, to date, been promised.

Additive manufacturing

AM technologies, known as rapid prototyping and solid freeform fabrication, are computer-directed layer-by-layer fabrication processes in which very thin layers of materials are stacked and adhered to shape a 3D physical model. AM technologies have been standardized and classified by the American Society for Testing and Materials International Committee F42 on AM Technologies into seven processes in accordance with the method of layers deposition and bonding, as described below [15].

Vat photopolymerization

Vat photopolymerization processes involve selective curing of predeposited photosensitive liquid polymer using light [15]. In stereolithography, the main vat photopolymerization technique, a laser beam or UV light source is used to project a cross-section of a single slice of the object onto a photopolymer resulting in the setting of the layer. This process is repeated until all the layers of the complete structure are created. Two-photon polymerization is a variation of the stereolithography process in which the photo initiator requires two photons to release a free radical that initiates polymerization; this approach results in significantly enhanced resolution.

Material extrusion

In this process, a continuous flow of materials in the form of paste or slurry is dispensed layer-by-layer using a 3D motion system incorporated with an extrusion nozzle. Material extrusion is diverse in concept but can be classified into two subgroups: processes based on material melting (comparable with fused deposition modeling, precision extrusion deposition [16], 3D fiber deposition [17] and multiphase jet solidification [18]) and processes without material melting (comparable with pressure-assisted microsyringe [19], 3D bioplotting [20], solvent-based extrusion freeforming [42], robocasting [21] and direct-write assembly [22]). Electrospraying describes the disruption of a liquid into a spray of charged particles when subjected to an intense electrical field, and was first described 25 years ago [23]. If the jet turns into very fine fibers instead of breaking into small droplets, the process is known as electrospinning. With the use of a coaxial needle comprising a central needle dispensing biological fluid containing cells and an outer needle dispensing biopolymer with low conductivity, electrospinning is capable of delivering viable cells [24] and active growth factors [25], as well as producing scaffolds with roughened surfaces to facilitate cellular migration [26] and control fiber orientation [27].

Material jetting

Material jetting is the use of inkjet printing or other similar techniques to deposit droplets of material that are selectively dispensed through a nozzle or an orifice to build the 3D structure. The material often turns into a solid subsequent to the deposition process via cooling (e.g., by crystallization or vitrification), chemical changes (e.g., through the cross-linking of a polymer) or solvent evaporation [20,33]. Commercial material jetting systems typically cure with a photopolymer ink using UV light in the inkjet printing process. In inkjet printing technology, two techniques are predominantly utilized for material droplet creation, namely, drop-on-demand and continuous inkjet.

Binder jetting

Binder-jetting techniques use nozzles to print material; however, instead of printing with the build material, the printed material is the 'glue,' which holds the powder together in the desired shape [15]. The 3D printing process is the main binder-jetting technique based on inkjet technology in which droplets of a binder material are deposited over the surface of a powder bed, adhering to the powder particles together where the part is to be shaped. The process is followed by lowering of the powder bed via a piston and a fresh layer of powder is then spread over the previous layer and, again, binder is deposited over the surface of the new layer. This procedure is repeated to build the whole structure.

Powder bed fusion

Powder-bed-fusion machines work in a manner similar to binder jetting; however, instead of printing glue onto a layer of powder, thermal energy is used to melt the powder into the desired pattern [15]. Most systems use laser power to melt the polymer, metal or ceramic material. Partial melting is termed selective laser sintering and full melting, selective laser melting. The application of an electron beam to melt the metal powder is known as electron beam melting. Finally, selective mask sintering offers a slightly different system that utilizes infrared light through a digitally printed optical mask to melt a thin layer of plastic powder.

Directed energy deposition

Directed energy deposition uses a laser beam to melt and fuse particles of the powder material delivered from the material deposition head. The X-Y table is moved to shape the cross-section of each desired layer. This process is repeated until all the desired cross-sectional layers of the structure are created. Other types of this technology are known as laser engineering net shape and direct metal deposition.

Sheet lamination processes

Sheet lamination techniques work by selective cutting and bonding sheets of material to form an object. The original system used glue or binder to bond paper or plastic sheets and is called Laminated Object Manufacturing (LOM), whereas ultrasonic welding of metal sheets is named Ultrasonic Consolidation (UC).

Table 1 summarizes specifications and applications of various AM processes.

Advances in the use of AM in trauma & orthopedic surgery

Clinical implants

The use of AM to produce permanent implants is outside the scope of this article. However, implants do demonstrate properties unique to AM, and in the case of cranio-maxillofacial implants, an area where the most clinical translation has occurred. These developments will be briefly reviewed. AM technologies can extract digital information from cross-sectional imaging routinely used in clinical practice such as computed tomography (CT)/MRI scans and apply this to build custom implants. The main advantages of AM technologies are manufacturing flexibility and the capability to fabricate implants of complex external shape and internal structures including the capacity to

Table 1. Classification and applications of different additive manufacturing techniques.

Process	Typical AM techniques	Advantages	Disadvantages	Applications	Living cells and growth factors	Experimental or commercial in medical field
Photopolymer vat	SL, 2PP	High-dimensional accuracy, offering transparent materials	Only photopolymers, single composition, cytotoxic photoinitiator, incomplete conversion thus postcuring required, limited cells for incorporation, nonhomogeneous cell distributions	Printing clinical implants and surgical guides, tissue engineering scaffolds, 3D micro-vasculature networks, biological chips, cell-incorporated 3D biological constructs	Yes	Experimental
Material extrusion	Melting extrusion: FDM, PED, MJS, 3D fiber deposition	Rapid, no toxic materials, good material properties	Low-dimensional accuracy, delamination, weak bonding between dissimilar polymers	Printing clinical implants, tissue-engineering scaffolds	No	Experimental
	Extrusion without melting: PAM, 3D bioplotting, solvent-based extrusion freeforming, robocasting, direct-write assembly, electrospinning	Simple and cheap mechanism, no trapped materials, low material waste, fairly high fabrication speed, cell-friendly environment	Relatively low-dimensional accuracy and mechanical strength, solvent is sometimes used, precise control of ink rheology is crucial	Printing tissue-engineering scaffolds, cell-incorporated 3D biological constructs, organ bioprinting	Yes	Commercial
Powder bed fusion	SLS, SLM, EBM, SMS	Wide range of materials, great material properties, high material strength	Thermal stress, degradation, accuracy limited by the particle size of materials, requirement for atmosphere control for metals	Printing surgical implants with complex internal and external structures, tissue-engineered scaffold, medical devices	No	Commercial
Directed energy deposition	LENS, DMD, LC	Wide range of materials, good material properties	Low-dimensional accuracy, thermal stress, requirement for atmosphere control, requirement for machining process for finishing the part	Printing orthopedic implants	No	Experimental

2PP: Two-photon polymerization; 3DP: 3D printing; AM: Additive manufacturing; DMD: Directed metal deposition; DoD: Drop-on-demand; EBM: Electron beam melting; FDM: Fused deposition modeling; LC: Laser cladding; LENS: Laser engineering net shape; LOM: Laminated object manufacturing; MJS: Multiphase jet solidification; PAM: Pressure-assisted microsyringe; PED: Precision extrusion deposition; PJT: PolyJet technology; SL: Stereolithography; SLM: Selective laser melting; SLS: Selective laser sintering; SMS: Selective mask sintering; UC: Ultrasonic consolidation.

Table 1. Classification and applications of different additive manufacturing techniques (cont.).

Process	Typical AM techniques	Advantages	Disadvantages	Applications	Living cells and growth factors	Experimental or commercial in medical field
Sheet lamination	LOM, UC	Low-temperature effects	Shrinkage, significant amount of waste, delamination	Printing orthopedic implants	No	Experimental
Material jetting	DoD inkjet printing, PJT	Rapid process, wide range of biomaterials, yet jettable materials, use of existing inexpensive technology, multiple compositions, multicell printing	Nozzle blockage an issue, low viscosity prevents build-up in 3D, low strength	Printing clinical implants and surgical guides, printing tissue-engineering scaffolds, printing cell incorporated biological constructs, organ bioprinting	Yes	Experimental
Binder jetting	3DP	Low-temperature process, rapid process, multiple compositions	Requirement of powder, high porosity, low surface quality, accuracy limited by the particle size of materials, powder entrapment, cell-challenging environment	Printing clinical implants and tissue-engineering scaffolds	No	Experimental

2PP: Two-photon polymerization; 3DP: 3D printing; AM: Additive manufacturing; DMD: Directed metal deposition; DoD: Drop-on-demand; EBM: Electron beam melting; FDM: Fused deposition modeling; LC: Laser cladding; LENS: Laser engineering net shape; LOM: Laminated object manufacturing; MJS: Multiphase jet solidification; PAM: Pressure-assisted microsyringe; PED: Precision extrusion deposition; PJT: PolyJet technology; SL: Stereolithography; SLM: Selective laser melting; SLS: Selective laser sintering; SMS: Selective mask sintering; UC: Ultrasonic consolidation.

create porous structures for weight reduction, tailoring stiffness and improving osteointegration. Critically, AM-manufactured implants accurately fit the defect site as the implant is developed from patient-specific digital data. In addition, an implant with a carefully designed lattice incorporating specific geometries confers the central advantage reducing stress shielding as the implant can closely match the stiffness of the bone. Moreover, material properties of AM-derived implants are normally better than investment-casted implants as the microstructure of the metal is finer resulting in higher tensile and flexural strengths [28].

Figure 2 depicts different 3D-printed clinical implants for use in reconstructive surgery.

Bone graft

The optimal properties of bone graft material include biological properties discussed previously, which encompasses control of porosity and the ability to match the graft to the defect site. As previous authors have stated the ideal bone graft substitute for all situations does not exist. Thus, with different clinical problems, different substitutes or combinations are required [30].

Allograft and autograft may be modified intraoperatively, but limitations on size, topography available and the ability to remodel fragments using an osteotome render accurate contouring of the graft to the defect site challenging. Traditional methods for the manufacture of synthetic bone graft, such as solvent casting/salt leaching, phase separation and foaming also have a number of limitations including shape restrictions, inconsistency and inflexibility, rendering these approaches poorly suited to produce graft material that accurately matched to the defect site. Klammert *et al.* were able to produce calcium phosphate implants precisely matching cranial defects mapped with the use of CT in an *ex vivo* model using AM [31]. The authors employed a binder-jetting process with phosphoric acid deposited onto tricalcium phosphate (TCP) powder that was subsequently hardened with additional phosphoric acid and subsequent autoclaving. Resulting material could be drilled, and held with plate and screw fixation as required. However, while demonstrating the ability of AM to delicately control graft topography, the pores remained smaller than the optimal size required and biodegradation was prolonged.

A key limitation of synthetic bone substitutes is the lack of control on porosity and pore interconnectivity, which are known to be of crucial importance in bone regeneration [32]. By contrast, AM offers delicate and exquisite control of these parameters, as well as other critical variables including filament size and alignment [33]. Extrusion-based AM is a technique that is particularly well suited to the formation of bone graft material. The additive nature of extrusion freeforming ensures minimal waste of biomaterial and makes this process suitable for mass production of tissue-engineering

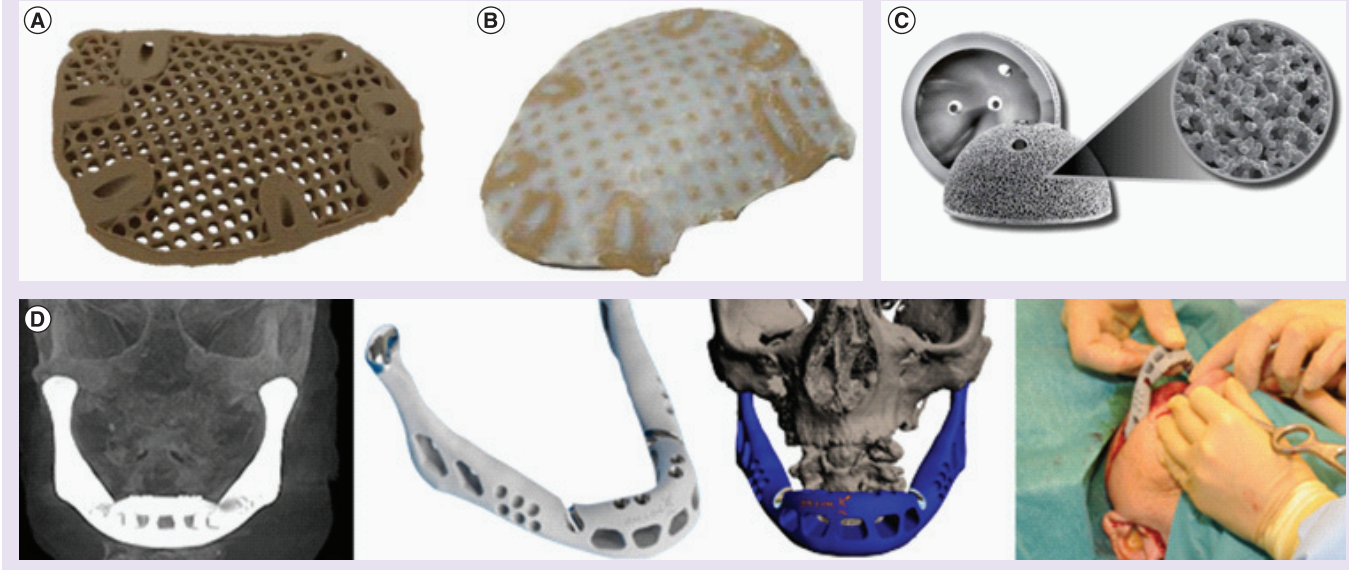

Figure 2. Examples of clinical implants produced using various additive manufacturing technologies for use in reconstructive surgery. **(A)** Cranial implant printed using selective laser sintering process from polyether ether ketone (PEEK) HP3 (PEEK material developed for use in selective laser melting EOS GmbH [Electro Optical Systems, Germany] sintering machine). **(B)** Infiltrated PEEK implant with a bioabsorbable polymer/hydroxyapatite hybrid material [29]. **(C)** An acetabular cup with porous surface printed using electron beam melting technology in a single process. **(D)** Total lower jaw implant in titanium printed by LayerWise using SLM process. **(C)** Figure courtesy of Arcam AB (Mölndal, Sweden); **(D)** Reproduced with permission from Layerwise NV (Leuven, Belgium).

scaffolds, multiple material porous bioactive structures [34] and microscale structures [13]. Solvent-based extrusion freeforming processes [35–37] have been successfully used for making high-resolution (<60-μm filament diameter) bioceramic scaffolds. Unique nozzle selection, paste formulation and paste rheological properties of this technique have enabled the finest ceramic scaffold fabricated using powder-based ceramic materials to be processed [38].

To circumvent the problems associated with the incorporation of growth factors or cells in AM, attempts have been made to enhance bone formation with the incorporation of silicate and metallic particles. Fielding and Bose investigated the osteoinductive potential of silicate and zinc oxide [39]. SiO_2 and ZnO particles were incorporated into β-TCP scaffolds produced using a binder-jetting technique and laser sintering. β-TCP scaffolds with and without SiO_2/ZnO particles were placed in rat femoral defects and subjected to a variety of tests including push-out testing, histology and micro-CT. Addition of SiO_2/ZnO particles was demonstrated to promote osteogenesis. This technique could represent a useful therapeutic strategy; however, given the significant problems resulting from metallic particulate matter stimulating immunological reactions following metallic hip implants [40], further investigation will be required.

Meseguer-Olmo *et al.* used silicate hydroxyapatite particles to enhance the osteoconductive ability of polycaprolactone (PCL) [41]. Hydroxyapatite and PCL were dispersed and dissolved using a solvent, and following printing, the scaffold was heated to 50°C overnight to ensure full evaporation of the solvent. Resulting scaffolds, alone or in combination with demineralized bone matrix, were implanted ectopically and orthotopically in rabbits. At 4 months, bone regeneration was seen in peripheral areas of all scaffolds using histology, while demineralized bone matrix appeared to promote bone regeneration centrally. While these results suggest the ability of this scaffold material to regenerate bone, the data would be further enhanced through comparison to control groups, as well as analysis using techniques such as CT.

Reichert *et al*. successfully used AM to produce bone graft material capable of mediating reconstruction of large bone defects [42]. Fused deposition molding of medical-grade PCL-TCP was used to produce cylindrical scaffolds. These scaffolds alone and in combination with BMP-7 or bone marrow cells were evaluated in a critical-sized defect in an ovine tibial model. Comparison was made with empty defects, and treatment representing the current clinical gold-standard, autologous bone grafting. The authors reported scaffolds combined with BMP-7 produced bone regeneration equivalent to autologous bone graft, while addition of bone marrow cells to scaffold material was not seen to augment bone formation. This ovine study including histological, biomechanical and micro-CT analysis at 3 and 12 months represents perhaps the closest to clinical translation attained, thus far, in the application of AM to treat large bone defects.

A current limitation with AM techniques to produce bone graft materials described above [31,39,41,42] remains the need to enhance cell and growth factor compatibility – currently limited by the application of thermal or chemical treatment. It is noteworthy that while Reichert *et al.* have demonstrated significant success in their technique, growth factor (BMP-7) and cells were applied as a separate process following production and sterilization of the scaffold [42].

Inkjet and extrusion-based AM systems such as 3D bioplotting can be used for simultaneous scaffold formation, cell and growth factor delivery when used under sterile conditions. Inkjet printing systems have previously been limited by loss of cell viability and cell/debris obstruction. Moon *et al*. were able to overcome these problems with the use of mechanical valves permitting printing of high-viscosity hydrogel precursors containing cells [43]. This bioprinting platform enabled synthesis of multilayered 3D hydrogel structures seeded with muscle cells at high densities, albeit with a dramatic reduction in resolution, with droplets >0.5 mm. While smooth muscle cells were used in this study, this technology could be applied to other cell types including bone marrow stromal cells. Other studies have also demonstrated the capability of AM to print complex 3D constructs containing multiple living cell types. Marga *et al.* reported bioprinting of multiple cell types (bone marrow and Schwann cells) and agarose cylinders to build a three-lumen tube using an extrusion-based bioprinter [44]. Xu *et al*. mixed human amniotic fluid-derived stem cells, canine smooth muscle cells and bovine aortic endothelial cells separately with ionic cross-linker calcium chloride [45]. Each cell type was dispensed from separate ink cartridges using a modified thermal inkjet printer (Figure 3B & C). The biological functions of the 3D-printed constructs were evaluated *in vitro* and *in vivo*. Critically, printed cell types maintained their viability, normal proliferation rates, phenotypic expression and physiological functions within the heterogeneous constructs.

Spinal fusion

Spinal fusion can be facilitated with the use of autologous bone graft, allograft or synthetic bone, alone or supplemented with bone marrow cells or osteoinductive factors. Fischer *et al.* performed a systematic analysis of the outcomes of these modalities and concluded that

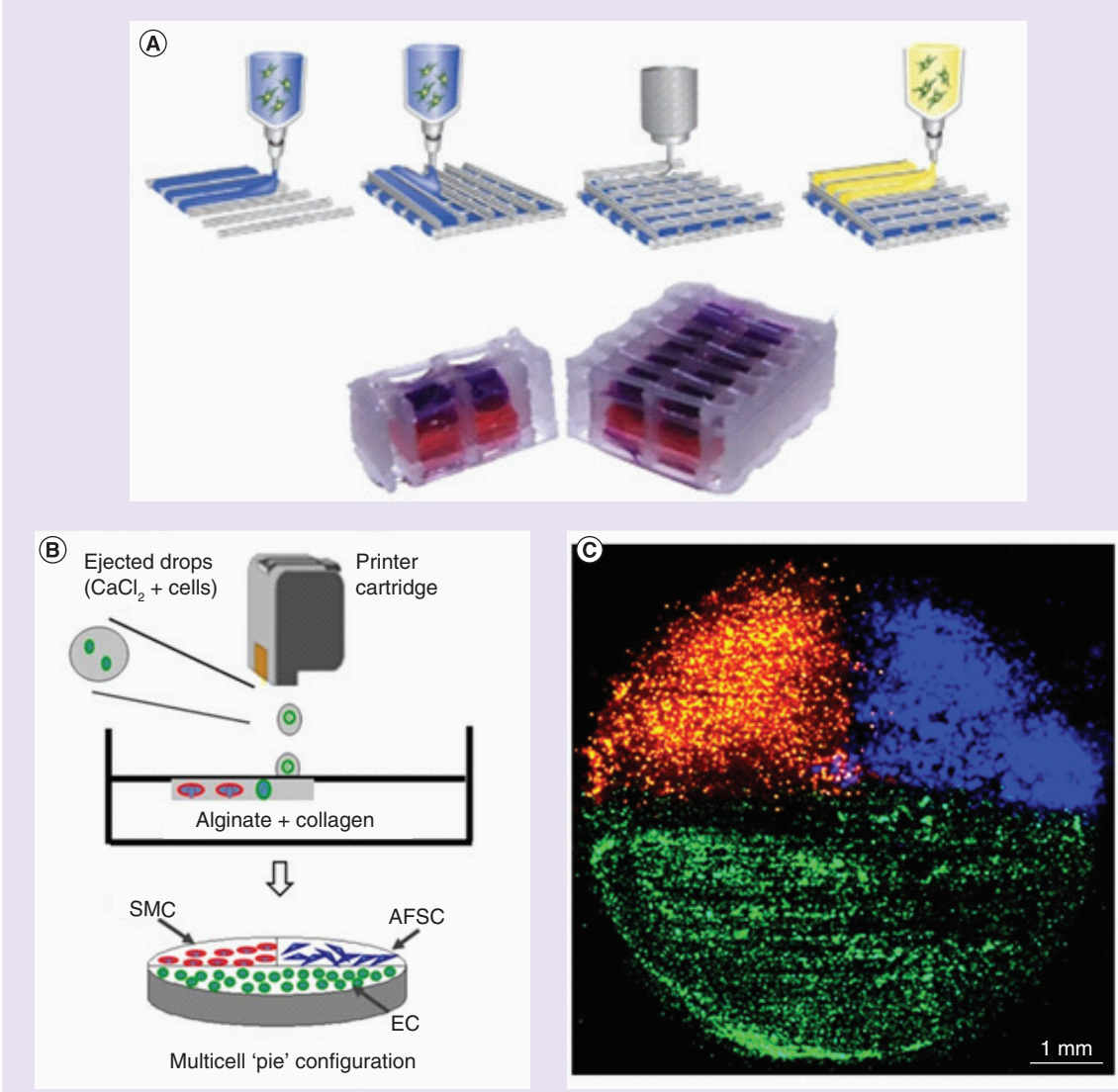

Figure 3. Biofabrication strategies adopted for direct 3D tissue printing. (A) Fabrication of solid biodegradable materials with cell-laden hydrogels: schematic illustration of a hybrid bioprinting process including alternating steps of printing biodegradable polymer and cell-laden hydrogels, and layering of the dye-containing alginate results in specific confinement of the printed hydrogels [46]. **(B)** 3D tissue constructs using simultaneous ink-jetting of multiple cell types. Human AFSCs, canine SMCs and bovine aortic ECs are separately mixed with ionic cross-linker $CaCl_2$, loaded into separate ink cartridges and printed using a modified thermal inkjet printer. The three cell types were delivered layer-by-layer to predetermined locations in a sodium alginate–collagen biocomposite located in a chamber under the printer. The reaction between $CaCl_2$ and sodium alginate results in a rapid formation of a solid composite gel and the printed cells are anchored in designated areas within the gel. The printing process is repeated for several cycles leading to a complex 3D multicell hybrid construct [45]. **(C)** Microscopic top views of a complete 3D multicell 'pie' construct before implantation. The cells that appear in green are bovine aortic ECs labeled with PKH 26 dyes; the cells that appear in blue are humanAFSCs tagged with CMHC dyes; the cells that appear in red are canine SMCs labeled with PKH 67 dyes [45].
AFSC: Amniotic fluid-derived stem cell; EC: Endothelial cell; SMC: Smooth muscle cell.
(A) Reproduced with permission from [46]. **(B & C)** Reproduced with permission from [45].
For color images please see www.futuremedicine.com/doi/full/10.2217/rme.14.20

the use of ceramics in combination with bone marrow aspirate showed a significant promise [7]. While limitations of current therapies include pseudoarthrosis and migration of cage devices, it should be acknowledged that in general terms levels of arthrodesis are high [7] and the correlation between arthrodesis and clinical outcome remains uncertain [47].

Abbah and colleagues sought to overcome the limitations of stress shielding and pseudoarthrosis by using fused deposition modeling to produce a

poly-ε-caprolactone scaffold with an internal fiber architecture, and compressive modulus specifically designed to match those of the cancellous bone [48]. Pore geometry was tailored to allow bone ingrowth. medical-grade PCL-TCP scaffold combined with BMP-2 demonstrated favorable outcomes compared with autologous bone grafting in a porcine model of lumbar interbody fusion. Furthermore, these results were supported by a recent study of medical-grade PCL with BMP-2 in a sheep thoracic spine fusion model [49].

Cage designs can lead to higher interference stresses and result in graft subsidence. In order to overcome this problem, Murphy *et al.* patented the concept of using AM to produce a biodegradable cage device in which the fixation plate could be integrated with the scaffold [50]. Devices based on this concept were designed for cervical interbody fusion and were produced using PCL. Additional PCL scaffolds were further modified with the inclusion of a calcium phosphate coating or collagen sponge containing BMP-7. These three scaffold types were then assessed in a porcine cervical fusion model [51]. In contrast to the other biodegradable scaffolds [52], these materials demonstrated sufficient mechanical strength for the 18-month duration of the experiment. Interestingly, the calcium phosphate coating and BMP-7 scaffolds demonstrated similar degrees of bone formation, both of which were superior to the unmodified PCL scaffold. Based on these findings, it may be hypothesized that coating of osteoinductive particles may circumvent the need for expensive and thermosensitive growth factors. Comparison of these scaffolds with a cage device incorporating autologous bone grafting would permit further evaluation of the effectiveness of this appealing strategy.

Osteochondral reconstruction

Tissue engineering approaches for the reconstruction of osteochondral defects can be described as a 'top-down' approach in which the scaffold is the key. The focus remains provision of a microenvironment to facilitate cell migration and differentiation. A polar opposite of this approach is the 'bottom-up' approach whereby scaffolds are eliminated, the rationale being that appropriate cells at high densities can produce the desired matrix [53]. Such scaffold-only [54] and cell-only techniques [55] represent two ends of a continuous spectrum with many authors employing a combination of cells, growth factors and scaffolds to facilitate tissue regeneration. In studies using cell delivery, controversy continues as to the cell type of choice, bone marrow stromal cells or chondrocytes [56,57], and in the case of chondrocytes if zonal isolation is important. Such a debate is beyond the scope of this article and has been detailed by others [57,58].

It is generally accepted that the zonal organization of type II collagen, chondrocytes and proteoglycans is of crucial importance to the function of articular cartilage [59]. It is also widely accepted that mechanical stimulation affects chondrocytes and synthesis of cartilage [60]. Scaffold pore size, pore geometry [61] fiber size [62] and pore interconnectivity [63] have all been shown to affect cartilage regeneration. Traditionally fiber size and porosity result from the choice of chemical or manufacturing process, whereas AM enables the specific selection of these parameters. Thus, AM enables production of scaffolds with specific variations porosity, enabling optimal properties to be elicited for specific regenerative requirements. Functionally graded nanocomposite structures [64] that are more suited to reconstruction at tissue interfaces such as osteochondral region can also be fabricated using AM.

Fedorovich *et al.* were able to dispense cells, control fiber spacing and the angle of deposition in 3D constructs produced using printing [65]. Heterogeneous scaffolds containing chondrocytes in alginate and bone marrow cells in alginate supplemented with biphasic calcium phosphate and hydroxyapatite were created. These constructs underwent *in vitro* culture or subcutaneous implantation in mice. The authors demonstrated heterogeneous tissue formation and the contribution of transplanted cells to extracellular matrix formation. Although this approach indicated a significant advance in the use of AM to produce tissue, the alginate material used is unlikely to confer sufficient mechanical strength to offer clinical translation without further modification.

Shim *et al.* used a six-nozzle extrusion system to form osteochondral tissue [66]. Two nozzles were heated and dispensed molten PCL to provide mechanical strength, while four nozzles dispensed a liquid alginate hydrogel at 20°C containing encapsulated human osteoblast-derived cells or chondrocytes derived from human nasal septum. The authors were able to control the porosity and left pores vacant in an attempt to enhance diffusion of oxygen to central areas of the construct. The study demonstrates the possibility of using AM to produce a porous scaffold seeded with two cell types with an assessed end point cell viability (live–dead stain) at 1 week. Successful tissue engineering will ultimately require that any incorporated cells are not only viable in the long term, but also remain in the chosen state of differentiation. The ability to maintain the cells in the desired state of differentiation is a recognized challenge in therapies targeting osteochondral injury [67], although timing of postoperative biopsy may also have an effect on tissue formation [68].

Cohen *et al.* have presented a novel concept for the *in situ* repair of osteochondral defects [69]. A modified

Fab@Home AM system was used to extrude alginate cross-linked with $CaSO_4$ prior to loading into a syringe and demineralized bone paste in a Gelatin carrier (BioSet™). The authors produced an alginate hydrogel and alginate-demineralized bone matrix plugs that matched the size and shape of defects formed on an *ex vivo* bovine femoral condyle. The requirement that the materials undergo cross-linking in a process compatible with the *in vivo* environment understandably places enormous limitations on the choice of materials, recognized by the authors. Materials that are dependent on laser, UV or chemical cross-linking to achieve phase deposition post printing are not suitable for *in situ* printing. Furthermore, in this specific case the paste must be of sufficient viscosity to enable retention of strength post extrusion, while sufficiently fluid to enable the material to pass through a relatively small needle. For ultimate clinical application, resolution of issues around porosity and mechanical composition (strength) will, thus, need to be addressed.

Periprosthetic infection

As discussed, standard therapy for deep infection in joint replacements involves removal of prosthesis, debridement, implantation of an antibiotic-impregnated cement spacer and, finally, revision to a definitive prosthesis following eradication of infection. In this treatment strategy only heat-stable antimicrobials can be used. Cement spacers are typically produced intraoperatively [77]; this takes time and may also result in a spacer of suboptimal dimensions. These temporary spacers are required to remain *in situ* for at least 2 months, and must be correctly formed to facilitate patient mobility and protect adjacent soft tissue. AM is capable of forming implants that provide a sustained release of heat-sensitive antibiotics [78]. As the amount of tissue debridement required in periprosthetic infection cannot be accurately determined by imaging, it is not likely that antibiotic spacers could be fabricated preoperatively for individual patients. However, AM could be used to produce an 'off-the-shelf' selection of spacers varying in size and topography, loaded with a selection of antibiotics. This could represent a clinically superior solution at reduced cost compared with current standard practice.

Other applications of AM

Several authors have reported on the use of additive manufacture to provide a 3D model to aide surgical planning [70] or form graft material to the specific clinical requirements [71,72]. Indeed, Lethaus *et al.* presented a study of 20 patients in which AM model mandibles were used to precontour plates to facilitate reconstruction [73].

Ongoing challenges in the use of AM in trauma & orthopedic surgery

Notwithstanding the tremendous progress in this field, key challenges are: vascularization of grafts, integration of the graft into surrounding tissue, sourcing of cells and growth factors, demonstration of long-term cell function, sterility, and ability to upscale production in an economically viable manner.

Vascularization

Construction of any tissue in excess of 100–200 μm in thickness requires a form of perfusion, preferably via a functioning vascular network to provide sufficient nutrient and gaseous exchange for the tissue [74]. Attempts have been made to incorporate pores within printed scaffolds to allow diffusion of adequate nutrients [66]. Miller *et al.* described the formation of a patterned vascular network in tissue material formed by AM [75]. A sugar-based template coated with a material to protect cells from osmotic damage was used to template the vascular network. This sugar-based material was subsequently removed revealing a tubular network, which was then seeded with human umbilical vein endothelial cells. While these strategies are innovative, the key will be the demonstration of a functional vascular network, comprised of endothelial cells that modulate permeability and direct cellular activity [76], surrounded by a muscle layer able to regulate flow. To date, a functional vascular network produced by any method remains to be fully demonstrated *in vivo*.

Cell source

Multiple studies have reported on the ability to use AM to distribute viable cells. These studies have typically explored viability at 1 week [66], although the long-term cellular viability remains undetermined. Studies of longer duration often do not include phenotypic or genotype analysis. In such cases, any damage to genetic material or changes in cell phenotype would not be manifest. This is of concern as studies have identified that even piezoelectric printing techniques can result in cell lysis [77]. In addition to the challenge of incorporating cell delivery into printing techniques, cells also need to be sourced. In the case of chondrocytes, this typically involves removal of 'donor' chondrocytes from a patient and *ex vivo* expansion. An alternative strategy may be use of bone marrow stromal cells obtained via intraoperative marrow aspiration. This approach has been successful in facilitating bone regeneration [78], spinal fusion [7] and osteochondral repair [79] in clinical studies.

Factors

Growth factors used, such as BMP-7, would also need to be sourced; typically the factors are expensive and

subject to a rapid decline in activity *in situ*. Following cell and growth factor preparation any printing process would have to be compatible with this biological material, performed in a sterile manner and on a timescale that maintains cell and or growth factor viability.

Barriers to commercialization of AM devices

While AM has been used to produce a range of products from implants to artificial organs, most of these applications have been developed through experimental systems; availability of commercial AM systems for biomedical applications is not that remarkable. Commercial AM systems developed primarily for industrial manufacturing purposes have been adapted or modified to perform specific applications in the medical sector. In the mainstay, these modifications are undertaken by biomedical research groups and institutes. Possibly the greatest obstacle to the commercial development of 3D printing applications is the lack of information and confidence of commercial AM systems suppliers in the biological performance of 3D-printed parts. This may, in part, be explained by the difficulty in demonstrating and validating predictable and reproducible biological viability of printed materials prior to and after biofabrication processes. To make current commercial AM systems suitable for use in orthopedic or advanced biomedical applications such as formation of tissue or artificial organs, a critical challenge is the modification of the process/device to enable processing of a wide range of biomaterials and to ensure a cell-friendly process environment. Current biofabrication processes such as extrusion-based systems in production of cell-seeded scaffolds may not offer satisfactory reproducibility. Similarly, production of precise tissue constructs with features less than 100 μm remains challenging, while integration of biomanufacturing systems with micro/nanosystems is limited due to the requirements for a clean environment. Furthermore, resulting specialized AM-based applications must meet stringent regulatory requirements, let alone be economically viable. In essence, evidence for biological performance, technical and regulatory challenges are the main barriers that need to be addressed in order to commercialize AM applications.

Future perspective

Bone graft

AM enables production of bone graft with biological and biomechanical features tailored for the particular clinical task. AM-fabricated bone graft is likely to achieve clinical superiority to allograft, and when combined with growth factors may indeed achieve efficacy equal to that of autograft in the near future.

Currently, the incorporation of growth factors and cells during printing severely limits the materials and processes that can be used and imposes significant logistical and time constraints (resulting material would require surgical placement prior to loss of biological activity). One potential economically and clinically viable solution remains the seeding of the bone marrow aspirate taken and delivered intraoperatively, and the delivery of growth factors frozen in a paste, which may be thawed and also delivered at time of surgery. Thus, a selection of 'off-the-self' sizes of graft material with tailor-printed graft used only in complex cases could benefit from this approach. An economically viable model may be the delivery, ultimately, of AM devices at level 1 trauma centers, or solely at a single national location. Electronic transmission of imaging files would permit remote fabrication of desired product and dispatch via a courier. Complex reconstructions requiring such graft material are generally planned in advance, and as such this system could provide the tailor-made graft in the requisite time.

Spinal arthrodesis

AM has been used to graft material of optimal biomechanical and biological properties for spinal arthrodesis, and has shown significant success in large animal models. When growth factors have been used, these factors have been applied intraoperatively following the production of the scaffold and this approach is likely to continue. While preoperative imaging offers the potential to produce patient-specific cage/fixation devices, such imaging cannot predict the amount of tissue tension or the amount of tissue that will be resected. For these reasons, and for cost control, it would seem likely that except for exceptional cases, a range of off-the-shelf products would be used rather than products produced for a specific patient.

Osteochondral reconstruction

In this clinical scenario, we envisage the predominant use of off-the-shelf products. While imaging may permit mapping of the defect size, it is unlikely to determine the health of surrounding tissue which may require debridement, leaving imaging unable to predict/map with accuracy the dimensions of the subsequently required graft. A role for *in situ* repair of defects is unlikely as the limitations on which materials can used are likely to outweigh potential advantages.

Models of orthopedic disease

While vascularization of tissue produced using AM is likely to remain a challenge for some time, we anticipate that AM may be harnessed to produce models of structural bone disease such as osteogenesis imperfecta, thus facilitating development of treatments. Printed tissue, such as bone, is also likely to partially replace animal testing in the pharmaceutical industry [80].

Financial & competing interests disclosure

The work of the authors is supported by a strategic longer and larger grant (sLOLA) from the Biotechnology and Biological Sciences Research Council, UK (BB/G010579/1) to R Oreffo, as well as partial funding from EU Biodesign (EU FP7) and Rosetrees Trust. M Vaezi has received funding from the Institute for Life Sciences, University of Southampton, and Invibio, UK. The authors have no other relevant affiliations or financial involvement with any organization or entity with a financial interest in or financial conflict with the subject matter or materials discussed in the manuscript apart from those disclosed.

No writing assistance was utilized in the production of this manuscript.

Executive summary

Additive manufacturing

- Additive manufacturing (AM) is an umbrella term encompassing a variety of techniques that involve computer-directed material fabrication in 3D.
- A variety of AM techniques have been successfully used to manufacture biocompatible scaffolds and to seed the scaffolds with viable cells.
- Cross-sectional imaging has been used to produce scaffolds that accurately match defect sites.

Advances in the use of AM in trauma & orthopedic surgery

- Surgeons have used AM to provide printed models to guide complex reconstruction and to produce graft material to match specific patient needs.
- Materials used in patients thus far remain far from optimal for application in long bone defects; however, evidence is emerging of the efficacy of such an approach including the demonstration of medical-grade polycaprolactone–tricalcium phosphate scaffolds combined with BMP-7 in a large animal model.
- AM-derived spinal fusion cages have been used with success in animal models; however, these cages are yet to translate into clinical practice.
- In general terms, AM will produce superior materials for a variety of clinical scenarios, but essentially, until new developments are forthcoming, growth factors and cells are likely to be applied intraoperatively rather than as part of the printing process.

Ongoing challenges in the use of AM in trauma & orthopedic surgery

- While presenting new opportunities, AM will need to address long-standing hurdles such as graft vascularization, cell and growth factor availability.

References

Papers of special note have been highlighted as:
• of interest; •• of considerable interest

1 Derby B. Printing and prototyping of tissues and scaffolds. *Science* 338(6109), 921–926 (2012).

2 Arafat MT, Gibson I, Li X. State of the art and future direction of additive manufactured scaffolds-based bone tissue engineering. *Rapid Prototyping J.* 20(1), 13–26 (2014).

3 Van der Stok J, Van Lieshout EMM, El-Massoudi Y, Van Kralingen GH, Patka P. Bone substitutes in the Netherlands – a systematic literature review. *Acta Biomaterialia* 7(2), 739–750 (2011).

4 Younger EM, Chapman MW. Morbidity at bone graft donor sites. *J. Orthop. Trauma* 3(3), 192–195 (1989).

5 Kurien T, Pearson RG, Scammell BE. Bone graft substitutes currently available in orthopaedic practice: the evidence for their use. *Bone Joint J.* 95-B(5), 583–597 (2013).

• **Review of bone graft substitutes in current clinical use.**

6 Cowan JA Jr, Dimick JB, Wainess R, Upchurch GR Jr, Chandler WF, La Marca F. Changes in the utilization of spinal fusion in the United States. *Neurosurgery* 59(1), 15–20 (2006).

7 Fischer CR, Cassilly R, Cantor W, Edusei E, Hammouri Q, Errico T. A systematic review of comparative studies on bone graft alternatives for common spine fusion procedures. *Eur. Spine J.* 22(6), 1423–1435 (2013).

• **Use of bone graft substitutes in spinal fusion.**

8 Beutler WJ, Peppelman WC Jr. Anterior lumbar fusion with paired BAK standard and paired BAK proximity cages: subsidence incidence, subsidence factors, and clinical outcome. *Spine J.* 3(4), 289–293 (2003).

9 Curl WW, Krome J, Gordon ES, Rushing J, Smith BP, Poehling GG. Cartilage injuries: a review of 31,516 knee arthroscopies. *Arthroscopy* 13(4), 456–460 (1997).

10 Bentley G, Biant LC, Vijayan S, Macmull S, Skinner JA, Carrington RW. Minimum ten-year results of a prospective randomised study of autologous chondrocyte implantation versus mosaicplasty for symptomatic articular cartilage lesions of the knee. *J. Bone Joint Surg. Br.* 94(4), 504–509 (2012).

11 National Joint Registry of England, Wales and Northern Ireland. Full 9th NJR Annual Report. www.njrcentre.org.uk

12 Parvizi J, Adeli B, Zmistowski B, Restrepo C, Greenwald AS. Management of periprosthetic joint infection: the current knowledge: AAOS exhibit selection. *J. Bone Joint Surg. Am.* 94(14), e104 (2012).

13 Vaezi M, Seitz H, Yang S. A review on 3D micro-additive manufacturing technologies. *Int. J. Adv. Manuf. Technol.* 67(5–8), 1721–1754 (2013).

14 Melchels FPW, Domingos MAN, Klein TJ, Malda J, Bartolo PJ, Hutmacher DW. Additive manufacturing of tissues and organs. *Prog. Polym. Sci.* 37(8), 1079–1104 (2012).

15 Stucker B. Additive manufacturing technologies: technology introduction and business implications. In: *Frontiers of Engineering: Reports on Leading-Edge Engineering from the 2011 Symposium*. The National Academies Press, Washington, DC, USA, 5–14 (2011).

16 Wang F, Shor L, Darling A *et al.* Precision extruding deposition and characterization of cellular poly-epsilon-caprolactone tissue scaffolds. *Rapid Prototyping J.* 10(1), 42–49 (2004).

17 Woodfield TBF, Malda J, de Wijn J, Péters F, Riesle J, van Blitterswijk CA. Design of porous scaffolds for cartilage tissue engineering using a three-dimensional fiber-deposition technique. *Biomaterials* 25(18), 4149–4161 (2004).

- **Characterization of additive manufacturing (AM) process for articular cartilage engineering.**

18 Greulich M, Greul M, Pintat T. Fast, functional prototypes via multiphase jet solidification. *Rapid Prototyping J.* 1(1), 20–25 (1995).

19 Vozzi G, Flaim CJ, Bianchi F, Ahluwalia A, Bhatia S. Microfabricated PLGA scaffolds: a comparative study for application to tissue engineering. *Mater. Sci. Eng. C Biomimetic Supramol. Syst.* 20(1–2), 43–47 (2002).

20 Landers R, Mulhaupt R. Desktop manufacturing of complex objects, prototypes and biomedical scaffolds by means of computer-assisted design combined with computer-guided 3D plotting of polymers and reactive oligomers. *Macromol. Mater. Eng.* 282(9), 17–21 (2000).

21 Cesarano J. A review of robocasting technology. In: *Solid Freeform and Additive Fabrication*. Dimos D, Danforth SC, Cima MJ (Eds). Materials Research Society, Warrendale, PA, USA, 133–139 (1999).

22 Smay JE, Gratson GM, Shepherd RF, Cesarano J, Lewis JA. Directed colloidal assembly of 3D periodic structures. *Adv. Mater.* 14(18), 1279–1283 (2002).

23 Hayati I, Bailey AI, Tadros TF. Mechanism of stable jet formation in electrohydrodynamic atomization. *Nature* 319(6048), 41–43 (1986).

24 Carter NA, Jayasinghe SN, Mauri C. Biosprayed spleen cells integrate and function in mouse models. *Analyst* 136(17), 3434–3437 (2011).

25 Qi H, Hu P, Xu J, Wang A. Encapsulation of drug reservoirs in fibers by emulsion electrospinning: morphology characterization and preliminary release assessment. *Biomacromolecules* 7(8), 2327–2330 (2006).

26 Ahn SH, Lee HJ, Kim GH. Polycaprolactone scaffolds fabricated with an advanced electrohydrodynamic direct-printing method for bone tissue regeneration. *Biomacromolecules* 12(12), 4256–4263 (2011).

27 Thomas V, Jose MV, Chowdhury S, Sullivan JF, Dean DR, Vohra YK. Mechano-morphological studies of aligned nanofibrous scaffolds of polycaprolactone fabricated by electrospinning. *J. Biomater. Sci. Polym. Ed.* 17(9), 969–984 (2006).

28 Gbureck U, Hölzel T, Klammert U, Würzler K, Müller FA, Barralet JE. Resorbable dicalcium phosphate bone substitutes prepared by 3D powder printing. *Adv. Funct. Mater.* 17(18), 3940–3945 (2007).

29 Manning L. Additive manufacturing used to create first laser-sintered cranial implant geometry. *Adv. Mater. Processes* 170(9), 33–36 (2012).

30 Janicki P, Schmidmaier G. What should be the characteristics of the ideal bone graft substitute? Combining scaffolds with growth factors and/or stem cells. *Injury* 42(Suppl. 2), S77–S81 (2011).

31 Klammert U, Gbureck U, Vorndran E, Rodiger J, Meyer-Marcotty P, Kubler AC. 3D powder printed calcium phosphate implants for reconstruction of cranial and maxillofacial defects. *J. Craniomaxillofac. Surg.* 38(8), 565–570 (2010).

32 Kuhne JH, Bartl R, Frisch B, Hammer C, Jansson V, Zimmer M. Bone formation in coralline hydroxyapatite. Effects of pore size studied in rabbits. *Acta Orthop. Scand.* 65(3), 246–252 (1994).

33 Kalita SJ, Bose S, Hosick HL, Bandyopadhyay A. Development of controlled porosity polymer-ceramic composite scaffolds via fused deposition modeling. *Mater. Sci. Eng. C* 23(5), 611–620 (2003).

34 Vaezi M, Chianrabutra S, Mellor B, Yang S. Multiple material additive manufacturing – part 1: a review. *Virtual Phys. Prototyp.* 8(1), 19–50 (2013).

35 Yang S, Yang H, Chi X *et al.* Rapid prototyping of ceramic lattices for hard tissue scaffolds. *Mater. Des.* 29(9), 1802–1809 (2008).

36 Yang H, Yang S, Chi X *et al.* Sintering behaviour of calcium phosphate filaments for use as hard tissue scaffolds. *J. Eur. Ceramic Soc.* 28(1), 159–167 (2008).

37 Yang HY, Thompson I, Yang SF, Chi XP, Evans JRG, Cook RJ. Dissolution characteristics of extrusion freeformed hydroxyapatite–tricalcium phosphate scaffolds. *J. Mater. Sci. Mater. Med.* 19(11), 3345–3353 (2008).

38 Lu X, Lee Y, Yang S, Hao Y, Evans JRG, Parini CG. Fine lattice structures fabricated by extrusion freeforming: process variables. *J. Mater. Process. Technol.* 209(10), 4654–4661 (2009).

39 Fielding G, Bose S. SiO2 and ZnO dopants in three-dimensionally printed tricalcium phosphate bone tissue engineering scaffolds enhance osteogenesis and angiogenesis *in vivo*. *Acta Biomater.* 9(11), 9137–9148 (2013).

40 Langton DJ, Joyce TJ, Jameson SS *et al.* Adverse reaction to metal debris following hip resurfacing: the influence of component type, orientation and volumetric wear. *J. Bone Joint Surg. Br.* 93(2), 164–171 (2011).

41 Meseguer-Olmo L, Vicente-Ortega V, Alcaraz-Banos M *et al. In-vivo* behavior of Si-hydroxyapatite/polycaprolactone/DMB scaffolds fabricated by 3D printing. *J. Biomed. Mater. Res. A* 101(7), 2038–2048 (2013).

42 Reichert JC, Cipitria A, Epari DR *et al.* A tissue engineering solution for segmental defect regeneration in load-bearing long bones. *Sci. Transl. Med.* 4(141), 141ra93 (2012).

•• **Successful demonstration of the application of AM in treatment of segmental bone defects in a large animal model.**

43 Moon S, Hasan SK, Song YS *et al.* Layer by layer three-dimensional tissue epitaxy by cell-laden hydrogel droplets. *Tissue Eng C Methods* 16(1), 157–166 (2010).

44 Marga F, Jakab K, Khatiwala C *et al.* Toward engineering functional organ modules by additive manufacturing. *Biofabrication* 4(2), 022001 (2012).

45 Xu T, Zhao W, Zhu J-M, Albanna MZ, Yoo JJ, Atala A. Complex heterogeneous tissue constructs containing multiple cell types prepared by inkjet printing technology. *Biomaterials* 34(1), 130–139 (2013).

46 Schuurman W, Khristov V, Pot MW, van Weeren PR, Dhert WJA, Malda J. Bioprinting of hybrid tissue constructs with tailorable mechanical properties. *Biofabrication* 3(2), 021001 (2011).

47 Park Y, Ha JW, Lee YT, Sung NY. The effect of a radiographic solid fusion on clinical outcomes after minimally invasive transforaminal lumbar interbody fusion. *Spine J.* 11(3), 205–212 (2011).

48 Abbah SA, Lam CXL, Hutmacher DW, Goh JCH, Wong H-K. Biological performance of a polycaprolactone-based scaffold used as fusion cage device in a large animal model of spinal reconstructive surgery. *Biomaterials* 30(28), 5086–5093 (2009).

•• **Assessment of spinal fusion cage produced by AM in a large animal model.**

49 Yong M, Brooker B, Labrom RD, Askin GN, Hutmacher D, Adam CJ. Biomechanical performance of polycaprolactone (PCL)-based scaffold with rhBMP-2 in a sheep thoracic spine fusion model. *Eur. Spine J.* 23(3), 650–657 (2014).

50 Tissue Regeneration Systems, Inc.: US20110282392 (2011).

51 LaMarca F, Flanagan CL, Tseng W-J *et al.*A new resorbable integrated cervical plate/cage fusion device modified with osteoconductive coating or osteoinductive factors: preliminary results in a pre-clinical Yucatan minipig model. http://tissuesys.com/trs_media/publications/Link%203.pdf

52 Krijnen MR, Mullender MG, Smit TH, Everts V, Wuisman PI. Radiographic, histologic, and chemical evaluation of bioresorbable 70/30 poly-L-lactide-CO-D, L-lactide interbody fusion cages in a goat model. *Spine* 31(14), 1559–1567 (1976).

53 Castro NJ, Hacking SA, Zhang LG. Recent progress in interfacial tissue engineering approaches for osteochondral defects. *Ann. Biomed. Eng.* 40(8), 1628–1640 (2012).

54 Kon E, Delcogliano M, Filardo G *et al.* A novel nano-composite multi-layered biomaterial for treatment of osteochondral lesions: technique note and an early stability pilot clinical trial. *Injury* 41(7), 693–701 (2010).

55 Park JS, Woo DG, Yang HN *et al.* Chondrogenesis of human mesenchymal stem cells encapsulated in a hydrogel construct: neocartilage formation in animal models as both mice and rabbits. *J. Biomed. Mater. Res. A* 92(3), 988–996 (2010).

56 Koerner J, Nesic D, Romero JD, Brehm W, Mainil-Varlet P, Grogan SP. Equine peripheral blood-derived progenitors in comparison to bone marrow-derived mesenchymal stem cells. *Stem Cells* 24(6), 1613–1619 (2006).

57 Reyes R, Pec M, Sánchez E, Del Rosario C, Delgado A, Evora C. Comparative, osteochondral defect repair: stem cells versus chondrocytes versus bone morphogenetic protein-2, solely or in combination. *Eur. Cell. Mater.* 25, 351–365 (2013).

58 Schuurman W, Klein T, Dhert W, Weeren P, Hutmacher D, Malda J. Cartilage regeneration using zonal chondrocyte subpopulations: a promising approach or an overcomplicated strategy? *J. Tissue Eng. Regen. Med.* doi:10.1002/term.1638. (2012) (Epub ahead of print).

59 Izadifar Z, Chen X, Kulyk W. Strategic design and fabrication of engineered scaffolds for articular cartilage repair. *J. Funct. Biomater.* 3(4), 799–838 (2012).

60 Grad S, Eglin D, Alini M, Stoddart MJ. Physical stimulation of chondrogenic cells *in vitro*: a review. *Clin. Orthop. Relat. Res.* 469, 2764–2772 (2011).

61 Jeong CG, Hollister SJ. Mechanical and biochemical assessments of three-dimensional poly (1, 8-octanediol-co-citrate) scaffold pore shape and permeability effects on *in vitro* chondrogenesis using primary chondrocytes. *Tissue Eng. A* 16(12), 3759–3768 (2010).

62 Li W-J, Jiang YJ, Tuan RS. Chondrocyte phenotype in engineered fibrous matrix is regulated by fiber size. *Tissue Eng.* 12(7), 1775–1785 (2006).

63 Miot S, Woodfield T, Daniels AU *et al.* Effects of scaffold composition and architecture on human nasal chondrocyte redifferentiation and cartilaginous matrix deposition. *Biomaterials* 26(15), 2479–2489 (2005).

64 Erisken C, Kalyon DM, Wang H. Functionally graded electrospun polycaprolactone and β-tricalcium phosphate nanocomposites for tissue engineering applications. *Biomaterials* 29(30), 4065–4073 (2008).

65 Fedorovich NE, Schuurman W, Wijnberg HM *et al.* Biofabrication of osteochondral tissue equivalents by printing topologically defined, cell-laden hydrogel scaffolds. *Tissue Eng. C Methods* 18(1), 33–44 (2011).

• **Production of osteochondral tissue equivalents using AM.**

66 Shim J-H, Lee J-S, Kim JY, Cho D-W. Bioprinting of a mechanically enhanced three-dimensional dual cell-laden construct for osteochondral tissue engineering using a multi-head tissue/organ building system. *J. Micromech. Microeng.* 22(8), 085014 (2012).

67 Peterson L, Minas T, Brittberg M, Nilsson A, Sjögren-Jansson E, Lindahl A. Two-to 9-year outcome after autologous chondrocyte transplantation of the knee. *Clin. Orthop. Relat. Res.* 374, 212–234 (2000).

68 Gikas PD, Morris T, Carrington R, Skinner J, Bentley G, Briggs T. A correlation between the timing of biopsy after autologous chondrocyte implantation and the histological appearance. *J. Bone Joint Surg. Br.* 91(9), 1172–1177 (2009).

69 Cohen DL, Lipton JI, Bonassar LJ, Lipson H. Additive manufacturing for in situ repair of osteochondral defects. *Biofabrication* 2(3), 035004 (2010).

70 Tam MD, Laycock SD, Bell D, Chojnowski A. 3-D printout of a DICOM file to aid surgical planning in a 6 year old patient with a large scapular osteochondroma complicating congenital diaphyseal aclasia. *J. Radiol. Case Rep.* 6(1), 31–37 (2012).

71 Li J, Hsu Y, Luo E, Khadka A, Hu J. Computer-aided design and manufacturing and rapid prototyped nanoscale hydroxyapatite/polyamide (n-HA/PA) construction for condylar defect caused by mandibular angle ostectomy. *Aesthetic Plast. Surg.* 35(4), 636–640 (2011).

72 Zhim F, Ayers RA, Moore JJ, Moufarrege R, Yahia L. Personalized implant for high tibial opening wedge: combination of solid freeform fabrication with combustion synthesis process. *J. Biomater. Appl.* 27(3), 323–332 (2012).

73 Lethaus B, Poort L, Böckmann R, Smeets R, Tolba R, Kessler P. Additive manufacturing for microvascular reconstruction of the mandible in 20 patients. *J. Craniomaxillofac. Surg.* 40(1), 43–46 (2012).

• **Describes clinical application of AM in maxillofacial surgery.**

74 Radisic M, Yang L, Boublik J *et al.* Medium perfusion enables engineering of compact and contractile cardiac tissue. *Am. J. Physiol. Heart Circ. Physiol.* 286(2), H507–H516 (2004).

75 Miller JS, Stevens KR, Yang MT *et al.* Rapid casting of patterned vascular networks for perfusable engineered three-dimensional tissues. *Nat. Mater.* 11(9), 768–774 (2012).

• **Concept of using a temporary template to produce a vascular network.**

76 Kanczler JM, Oreffo RO. Osteogenesis and angiogenesis: the potential for engineering bone. *Eur. Cell. Mater.* 15, 100–114 (2008).

77 Cui X, Dean D, Ruggeri ZM, Boland T. Cell damage evaluation of thermal inkjet printed Chinese hamster ovary cells. *Biotechnol. Bioeng.* 106(6), 963–969 (2010).

78 Zimmermann G, Moghaddam A. Allograft bone matrix versus synthetic bone graft substitutes. *Injury* 42, S16–S21 (2011).

79 Nejadnik H, Hui JH, Choong EPF, Tai B-C, Lee EH. Autologous bone marrow-derived mesenchymal stem cells versus autologous chondrocyte implantation: an observational cohort study. *Am. J. Sports Med.* 38(6), 1110–1116 (2010).

80 Wüst S, Müller R, Hofmann S. Controlled positioning of cells in biomaterials – approaches towards 3D tissue printing. *J. Funct. Biomater.* 2(3), 119–154 (2011).

Review

For reprint orders, please contact: reprints@futuremedicine.com

Regenerative Medicine

Tissue engineering advances in spine surgery

Melvin C Makhni*[,1], Jon-Michael E Caldwell[1], Comron Saifi[2], Charla R Fischer[2], Ronald A Lehman[1], Lawrence G Lenke[2] & Francis Y Lee[1]

[1]Department of Orthopedic Surgery, New York-Presbyterian Hospital, Columbia University Medical Center, New York, NY 10032, USA

[2]The Spine Hospital, Department of Orthopedic Surgery, New York-Presbyterian Healthcare System, Columbia University Medical Center, 5141 Broadway, New York, NY 10034, USA

*Author for correspondence: mcm2225@cumc.columbia.edu

Autograft, while currently the gold standard for bone grafting, has several significant disadvantages including limited supply, donor site pain, hematoma formation, nerve and vascular injury, and fracture. Bone allografts have their own disadvantages including reduced osteoinductive capability, lack of osteoprogenitor cells, immunogenicity and risk of disease transmission. Thus demand exists for tissue-engineered constructs that can produce viable bone while avoiding the complications associated with human tissue grafts. This review will focus on recent advancements in tissue-engineered bone graft substitutes utilizing nanoscale technology in spine surgery applications. An evaluation will be performed of bone graft substitutes, biomimetic 3D scaffolds, bone morphogenetic protein, mesenchymal stem cells and intervertebral disc regeneration strategies.

First draft submitted: 7 September 2015; Accepted for publication: 8 January 2016; Published online: 12 February 2016

Keywords: biomimetic • bone graft • bone morphogenetic protein • disc regeneration • scaffolds • spine • stem cells • surgery • tissue engineering

Bone autograft remains the gold standard of bone graft materials due to their intrinsic osteoconductive, osteogenic and osteoinductive properties, low risk of immunologic reaction, and excellent mechanical stability. Bone is the most commonly transplanted biological material after blood with over 800,000 grafts implanted annually [1,2]. In orthopedic surgery, autografts include bone, tendons and ligaments. Despite the advantages of autografts, they are limited by a finite supply of donor tissue, donor site morbidity, pain, hematoma formation, nerve and vascular injury, and fracture [3–5].

Some of these limitations have been overcome by the increasingly common use of live or cadaveric donor bone allografts, used in over a third of bone graft surgeries [6]. Allografts are commonly considered the next best option after autografts and are available in multiple processed forms. While more readily available and without the donor site problems associated with autografts, allografts introduce unique problems including a reduced osteoinductive capability relative to autograft, lack of osteoprogenitor cells, increased risk of immune reaction, and perhaps most notably, a small risk of disease transmission [2,7,8]. Thus, a demand exists for tissue-engineered constructs that can provide the elemental requirements for bone regeneration while avoiding the complications associated with human tissue grafts.

Two major goals of spine surgery are eliminating degenerated intervertebral discs, and promoting bony fusion across vertebral segments. Currently degenerated discs cannot be reliably restored in the clinical setting, so surgery seeks to remove or eliminate them through bony fusion across them. However, tissue-engineered advances seek to shift this paradigm by offering strategies to restore the intervertebral discs or their component segments.

Future Medicine part of fsg

This review will focus on recent advancements in tissue-engineered bone graft substitutes and disc regeneration strategies that make use of nanoscale technology in spine surgery applications. An evaluation will be performed of bone graft substitutes, biomimetic 3D scaffolds, bone morphogenetic protein and mesenchymal stem cells (MSCs) formulations. Additionally, promising developments in tissue engineering strategies for intervertebral disc regeneration will be explored.

Bone graft substitutes

Bone graft substitutes have developed to circumvent the primary reliance on autograft to achieve bony fusion. Demineralized bone matrix and ceramics developed but have had results short of autograft, likely due to their lack of inherent properties of autograft that help create ideal fusion environments. Ceramics have opened new avenues for potential bone graft substitutes but are yet to show superior preclinical results.

In order to provide the optimal healing conditions for general clinical applications or as a tissue engineering scaffold, a bone graft substitute must possess the following qualities (Table 1): biocompatibility, biomechanical stability, osteoinductivity, an osteoconductive porous matrix and biodegradability (if the construct is intended to degrade over time) [9,10]. Multiple strategies for developing such devices have been developed using a wide array of materials and approaches. These materials have been deployed in various forms to aid in spinal fusion and fracture nonunion. Hence bone graft substitutes can be utilized either directly in clinical applications or as a tissue engineering scaffold.

Demineralized bone matrix (DBM) is acid decalcified cortical bone allograft that is then sterilely processed. The demineralization and sterilization process greatly reduces the mechanical strength of the material, but retains the trabecular structure of the original bone and some growth factors making it both osteoconductive and slightly osteoinductive due to varying concentrations of bone morphogenetic protein [11]. DBM has been extensively studied since it was first described by Urist and is a well-described substitute for and expander of bone autograft [12]. In many commercially available products, DBM is added to autograft, allograft, bone marrow aspirate, collagen or polymer carriers, ceramics, or growth factors to create a hybrid material with desirable biologic and structural properties. Recently, Baumann *et al.* retrospectively examined 101 patients with posterolateral instrumented fusions using DBM as a fusion expander and found a fusion rate of 94%, similar to that of autologous bone graft [13]. Ajiboye *et al.* demonstrated successful solid fusion in 84% of elderly patients following posterolateral interbody fusion with DBM combined with bone marrow aspirate in spite of concerns for reduced fusion potential in this population [14].

Ceramics comprise a major type of bone graft substitutes, which can be utilized as a scaffold for tissue-engineered bone. The microstructure of ceramic composites is similar to the mineralized phase of bone and these materials are both osteoconductive and biocompatible. They are also inert substances with a long storage life, are available in unlimited supply, and carry no risk of disease transmission [15]. However, ceramics have no osteogenic or osteoinductive capability, they persist in the body due to slow degradation, and mechanically they are brittle and stiff which increases the risk of fracture after cyclic loading [11,16–18]. Typically used ceramics include mono-, bi- and tri-calcium phosphate as well hydroxyapatite which can be used alone or combined with collagen, polymers, gels and other carrier materials to make cements [19,20]. When compared with gold-standard iliac crest bone graft in the setting of posterolateral fusion, coralline hydroxyapatite derived from sea coral yielded poorer to equivalent fusion rates [21,22]. Calcium phosphate has been reported to achieve fusion rates at 33 months up to 87% (vs 90% for iliac crest bone graft), but is associated with inflammation and wound drainage in up to 51% of patients [23,24]. Beta

Table 1. Characteristics of an ideal bone graft substitute or tissue-engineered scaffold.

Characteristic	Description
Biocompatibility	The material does not elicit an immune response from the host
Biomechanical stability	Permits secure fixation to the bone and withstands or transmits applied loads to surrounding bone
Osteoinductivity	Ability to contain or release growth factors, cells and other bioactive substances of interest
Osteoconductive porous matrix	Composed of a permeable material and structure that allows vascular ingrowth, cellular migration and cell to cell communication
Biodegradability	If the construct is intended to degrade over time, it should do so in a controlled manner into nontoxic metabolites that are not immunogenic

tri-calcium phosphate combined with autograft or allograft has been reported to achieve fusion rates up to 100% at 3 years following posterolateral fusion [25]. The fusion rates of these studies are difficult to interpret, even on computed tomography, since ceramic substitutes and bone have the same density on radiographs and CT. Thus, a ceramic substance may be mimicking a true bony fusion.

Recently, porous scaffolds have been developed using ceramics processed through foaming or other techniques to create a 3D, highly porous ceramic structure [10,26,27]. These scaffolds can have varying pore sizes to encourage cellular migration, osteointegration, and bony substitution and may prove to provide superior clinical results to current ceramic bone graft substitutes, which are primarily used as bone graft extenders.

Bioglass was originally developed in the 1970s as a novel ceramic that binds to bone [28]. The material forms a hydroxycarbonate apatite layer that has been shown to have osteoinductive as well as osteoconductive effects as it breaks down. The advent of thermally induced phase separation (TIPS; described below), foaming and additive manufacturing techniques have allowed Bioglass to be combined with polymers and processed into porous 3D scaffolds in the laboratory [29–31]. These scaffolds have a porous structure that could not be achieved through conventional manufacturing. Preclinical trials have shown that while the increased porosity of these structures improves osteoinduction and resorption, it comes at the expense of mechanical strength [32]. Lee *et al.* demonstrated in a rabbit model of lumbar fusion that certain formulations of bioactive glass can resorb too rapidly, before bone formation can occur, leading to inferior fusion results relative to autograft controls [33].

Biomimetic 3D scaffolds

Tissue engineering techniques such as electrospinning, TIPS and solid freeform fabrication (SFF) have allowed development of customizable scaffolds by circumventing inherent limitations in material designs. Mineralized collagen matrix has already shown initial promise in preclinical and clinical testing.

Unlike many bone graft substitutes that rely on only their material properties to augment bone healing, the next generation of 3D scaffolds offers tissue engineers the ability to optimize macro- and microstructural features. While these devices are still in the preclinical phase of development, *in vivo* studies have shown promising results. Many techniques exist to fabricate a fully engineered 3D scaffold, but the most commonly used are electrospinning, TIPS and SFF. These methods can be applied to a wide variety of synthetic, natural or hybrid materials with the ability to design devices on the nanoscale.

Electrospinning is a commonly used technique to produce nano- to micro-scale fibers. This technique produces a fabric-like sheet of fibers which can be highly aligned or random depending on the intended design. Multiple sheets can be stacked or interspersed with other materials to produce 3D constructs; however, recent modifications to this technique have allowed the formation of relatively thicker spongiform mats [34]. A number of different polymers can be used with electrospinning such as the biodegradable polyesters: poly(DL-lactic acid) (PDLLA), poly(glycolic acid) (PGA), poly(lactic-co-glycolic acid) (PLGA) and polycaprolactone (PCL) [31,35–40]. As a class, these versatile polymers offer predictable rates of degradation, are biocompatible and are US FDA approved for a number of specific indications. Pure polymers can also be combined with ceramics or other adjuvant materials.

TIPS operates on the principal that at low temperatures, polymer solutions become unstable and separate into two phases: one which is polymer-lean and one which is polymer-rich. The polymer-rich phase is extracted and the solvent removed, causing the polymer to solidify and create interconnected porous polymer foams with a nanofibrous structure [41]. Fibers can vary between 50 and 500 nm in diameter with a porosity as high as 98% [42]. This technique can also be combined with various porogens such as sugar, wax, salts and other dissolvable solids that are removed after polymer solidification to modify the shape and size of the resulting pores [40,43–45].

SFF, also known as 3D printing or additive construction, uses a digital 3D model to guide a computer-operated printer. The model can be designed *de novo* or based on a patient's CT or MRI images [41]. The printer itself can use various techniques to create the modeled object including heat-melt, laser sintering, photoactivation and others depending on the nature of the desired material. The resolution of these devices has increased dramatically in recent years with some systems boasting accuracy to the nanometer level. Similarly, reverse SFF can be used to create a negative mold of the desired object. This mold can then be used with other fabrication techniques like TIPS to create a scaffold with a defined nanofibrous microstructure as well as a molded macrostructure [46].

Mineralized collagen matrix (MCM) is a commercially available biomimetic matrix that has been used successfully as a bone graft substitute in the treatment of various orthopedic fractures as well as spine fusion [47,48]. This technology coats crosslinked type I collagen fibrils with hydroxyapatite resulting in a porous, osteoconductive 3D scaffold which is then

typically combined with osteoprogenitor cells from bone marrow aspirate. Khoueir *et al.* showed clinical improvement in 49 out of 60 patients treated with MCM following anterior cervical discectomy and fusion (ACDF) at 18 months [49]. Similarly, Yu *et al.* found identical clinical outcomes and fusion rates as well as improved surgical times and blood loss when using MCM as compared with autologous iliac crest bone graft [50].

rhBMP

Bioengineered substrates, primarily rhBMP, have passed the rigors of clinical testing and gained widespread acceptance and use throughout various aspects of spine surgery. These products, delivered through a variety of vehicles, have shown efficacy for certain indications; however recent analysis has shown that these benefits come with certain risks which are becoming increasingly recognized.

The first clinically available biologic therapy to promote spine fusion is rhBMP. rhBMP-2 and rhBMP-7 have each been FDA approved for specific spinal fusion procedures. However rhBMP-2 in particular, has been used widely for off-label spinal fusion procedures. Although widely acclaimed initially in the literature, significant warnings have emerged about possible complications of these bioengineered substitutes.

Rh-BMP-7, marketed as OP-1 by Stryker, was FDA approved in "compromised patients requiring revision posterolateral lumbar spinal fusion for whom autologous bone and bone marrow harvest are not feasible or expected to promote fusion." Compromised patients would include those with osteoporosis, diabetes and smokers. rh-BMP-7 is also indicated for long bone nonunions.

Recombinant hBMP-2 on an absorbable collagen scaffold, sold as INFUSE® (Medtronic, Dublin, Ireland) in conjunction with either the LT-Cage Lumbar Tapered Fusion Device or the Inter Fix RP Threaded Fusion Device is FDA approved for "spinal fusion procedures in skeletally mature patients with degenerative disc disease at 1 level" from L2-S1 in patients with no worse than grade 1 spondylolisthesis. The cage devices are designed to be implanted using a laparoscopic or anterior approach. Application of rhBMP-2 through a posterior approach with either transforaminal lumbar interbody devices or simply for posterolateral fusions without use of a cage is considered off-label use. Additionally, rhBMP-2 is approved for use in acute, tibial shaft open fractures as well as for maxillofacial regenerative use [51,52].

Recent re-examination of industry-funded rhBMP clinical trials by the Yale Open Data Access project has ignited controversy regarding the safety and efficacy of BMP [53,54]. Sponsored by Yale University with cooperation and funding from Medtronic, two groups independently analyzed the entirety of the study data supporting the use of INFUSE. The authors demonstrated a 12% higher fusion rate in patients with BMP used. At 6 months, there was a slightly increased relative risk of pain in the rhBMP-2 group, and then the relative risk of pain is lower in the rhBMP-2 group up to 2 years. They could not make any significant conclusions regarding adverse events due to the wide confidence intervals, but there were higher rates in the rhBMP-2 groups [53]. Additionally, the Yale Open Data Access groups found that the original studies were limited by reporting bias and adverse events were under-reported [53,54]. Significant adverse events have been reported with the use of BMP-2 in spinal fusion including increased incidence of cancer, retrograde ejaculation and sterility in men, vertebral osteolysis, postoperative radiculitis, and symptomatic ectopic bone formation [55,56].

Mesenchymal stem cells

Clinical applications of stem cell treatments remain in their infancy in spine surgery. Few applications exist currently, and these have limited data to support their efficacy. Since the development of rhBMPs, new biological materials incorporating stem cells have been clinically implemented. Osteocel™ by Nuvasive (CA, USA), incorporates allogenic MSCs and bone marrow-derived osteoprogenitor cells with demineralized bone and a cancellous scaffold [57]. A retrospective, single-surgeon case series of 52 consecutive patients undergoing lumbar interbody fusion for nontraumatic etiologies showed successful radiographic fusion rates of 92.3%, and an average follow-up of 14 months. Plain radiographs, as well as CT scans that were available for 52 patients, were utilized to determine the 7.7% pseudoarthrosis rate by noting lack of bone bridging at the fusion site. One patient had a wound infection, with a complication rate of 1.9%, which completely healed after nonoperative treatment. This study suggests a high rate of fusion comparable to that encountered with BMP and autograft, although no clinical data were presented [58].

Another retrospective case series was reported on Osteocel Plus™ in 23 patients undergoing minimally invasive, transforaminal lumbar interbody fusion. The authors demonstrated a 91.3% radiographic union rate. They reported two nonunions, one that was lost to follow-up and one that declined revision surgery. They reported no other complications attributable to the Osteocel Plus substrate [59]. Numerous other tissue-engineered constructs continue to be under development, although none have made it into clinical use.

Intervertebral disc regeneration

Development of strategies for intervertebral disc regeneration represents a paradigm shift in the management of disc degeneration. Traditional treatments involved removing damaged discs, while recent technologies such as disc replacement seek to maintain motion at these disc segments but still through removal of the affected discs. Newer strategies focusing on biologic disc regeneration have been attempted but are yet to show clinical efficacy.

Tissue engineering initially brought bone regeneration products to market, but attempts are being made at intervertebral disc (IVD) components. Classically, disc degeneration has been treated with resection of the incompetent tissue for pain relief, instead of restoration of native anatomic architecture. Recently, disc arthroplasty has been FDA approved for use in single level L4-L5 or L5-S1 segments with satisfactory short-term results in select cases of degenerative disc disease [60–64]. The Prodisc-L™ implant (DePuy Synthes, PA, USA) yielded improvements in disc height and motion, return to work, pain and satisfaction seen as early as 3 months postoperatively, and being maintained through the 2-year study period [60]. At 2-year follow-up, these lumbar arthroplasty devices have had superior subjective and objective functional outcomes than traditional fusion without any major complications [65]. Two level implants have recently enjoyed similar short-term success. A recent meta-analysis by Yao *et al.* comparing total disc arthroplasty with anterior cervical discectomy and fusion for cervical degenerative disease found disc arthroplasty to have better overall success, better neurological success and lower incidence of second surgical procedures relative to ACDF [66].

Biologic methods of regenerating and repairing native disc tissue such as native or engineered DNA, signaling molecules, scaffolds, and carriers which seek to reconstitute both the nucleus pulposus and the annulus fibrosus are under study. Initially, tissue transplantation was attempted, with the goal of transferring autogenous and allogeneic disc material. However, the availability of tissue remained a limiting factor and *in vitro* culturing of tissue failed to maintain the integrity of the tissue. Allograft tissue also has the potential for host rejection and disease transmission.

Preclinical trials have researched the impact of implanting cells, scaffolds, chemical signals or a combination of these for disc regeneration in animal models. Autologous disc chondrocyte transplantation (ADCT) has been attempted in humans through the prospective, randomized, multicenter Eurodisc trial [67,68]. This trial reported promising evidence that these cells could be harvested and cultured, then returned to individuals safely, and could also reduce pain in at least the short term. Despite initial hopeful results in this and other early trials, no intervention has been proven to be rigorous enough to be approved for therapeutic use in humans. Of the 112 patients enrolled into the Euro Disc trial, 28 were evaluated at 24 months and found to have small but statistically significant improvements in pain. On a 100-point visual-analog pain scale, the ADCT patients improved 48 points as compared with 42 points across the study time horizon. Although they showed similar disc heights on MRI, there was a 1.6-fold higher normal fluid content in the affected discs after ADCT treatment at 2-year follow-up [69].

Nucleus pulposus

Efforts to address deficiencies in the nucleous pulposus portion of the intervertebral disc have shown promise in preclinical trials. Native biologics in combination with gene therapy, stem cells and microparticle delivery may help to restore native architecture of the nucleus pulposus.

The goal of nucleus pulposus therapy is to prevent disc space collapse as well as replace disc material to aid in proper function of the intervertebral disc. Tissue engineering approaches to nucleus pulposus regeneration have utilized molecular and mechanical signals, cells and scaffolds. Growth factors can be delivered directly to the nucleus pulposus or through vectors promoting their delivery. Various proteins have been delivered, such as TGF-β, FGFs, BMPs and growth differentiation factors (GDFs) [70,71]. One of these GDFs, GDF-5 has produced promising results in animal models to combat the deteriorative effects of degenerative disc disease. Basic science studies as well as preclinical studies in murine and bovine models have shown restoration of cellular and matrix integrity of the extracellular matrix attributed to the presence of GDF-5 [72,73]. Disc height has even been shown to improve in degenerative disc disease models after an injection of GDF-5, while injections of various other growth factors did not seem to confer the same benefit [74]. Both BMP-7 and GDF-5 have been FDA approved for use in clinical trials [75]. Intradiscal rhGDF-5 is currently being evaluated by DePuy Spine in early clinical trials for use in humans [76].

The goal of cellular delivery to the nucleus pulposus is to facilitate restoration of extracellular matrix proteins. Both chondrocytes and MSCs have the potential to produce collagen and proteoglycans, and are targets for use in degenerative nucleus pulposus models. Human adipocyte-derived stem cells (ADSCs) have been differentiated into cells that mimic those in the nucleus pulposus when they were cocultured with nucleus pulposus cells, and produced elevated levels of

nucleus pulposus matrix proteins such as collagen and proteoglycans [77–79]. Additionally, combining ADSCs and *GDF-5* has also shown beneficial results. *TGF-β* and GDF-5 genes were independently transduced via adenoviral vectors into rat ADSCs, and both cell lines showed increased staining of nucleus pulposus components such as proteoglycans and type 2 collagen which suggests improvement in restoring native nucleus pulposus architecture [80]. Similarly, Sox9-transduced bone marrow MSCs were shown to have enhanced chondrogenic differentiation and preservation of nucleus pulposus (NP) structure in a rabbit model [81]. Implantation of allogeneic cells into degenerative nucleus pulposus in a rabbit model showed not only higher type II collagen content and decreased histologic degeneration, but also no evidence of immunologic rejection [82].

Various biomaterial scaffolds have been used to heal nucleus pulposus degeneration [83,84]. Chitosan, a modification of a compound found in crustacean shells known as chitin, is a biocompatible, biodegradable material that has been used successfully in recent preclinical studies [85–87]. It can be converted into a thermosensitive hydrogel that solidifies when injected into the disc and at physiological temperature. It has been shown to maintain bovine nucleus pulposus cells as well as differentiate human MSCs toward nucleus pulposus cells [88–90]. Additionally, scaffolds in the nucleus pulposus can be functionalized by bonding them to heparin in order to enhance binding to growth factors. This can be done through covalently bonding them to heparin, or by grafting microparticles containing heparin onto the scaffolds [91–93]. This can result in enhanced attachment of MSCs to the scaffold [94]. Scaffolds can also be modified to allow for controlled release of growth factors such as FGF-2, which can further aid in nucleus pulposus revitalization [95].

Annulus fibrosus

Intact annulus fibrosus is crucial in retaining the nucleus pulposus within it. Various strategies of recreating aspects of the annulus, as well as adhering to it as a patch over defects, may provide novel means to prevent extrusion of disc contents.

The axial load absorption of the disc is capable due to the confinement of the nucleus pulposus by the surrounding annulus fibrosus, which must retain the ability to regain its native shape after deformation [70]. Cell-based strategies have been implemented to transplant primarily mesenchymal stromal cells to the target region in the disrupted annulus fibrosus [96,97]. Although only a small portion of the transplanted cells remains viable in the location they are injected after a few days, cellular transplantation may be able to decrease subsequent cellular degeneration as well as improve tissue regeneration at the target site [98–102].

Scaffolds designed with strong materials such as polyglycolic acid and polylactic acid have been enhanced to optimize both mechanical properties and biocompatibility [103–105]. Increasing polylactic acid yielded polymers with increased compressive modulus, but concurrently decreased cell binding ability. The cells attached to the polyglycolic acid were also shown to possess flatter morphology as compared with the rounder cells attached to the polylactic acid.

Newer methods of electrospinning have been able to recreate the native multilayered morphology of the annulus fibrosus. Poly(e-caprolactone) has been electrospun with good geometric precision [106–108]. Silk is another material that not only can be electrospun into fibers to recreate the annulus fibrosus, but also possesses toughness appropriate for use in the annulus fibrosus. Silk scaffolds are also a promising material to be able to incorporate well with and attach to bovine annulus fibrosus cells [109,110]. Annulus fibrosus is composed primarily of collagen, so numerous studies have analyzed various forms of predominantly collagen matrices to serve as annulus fibrosus substitutes [111–113]. Huang *et al.* seeded nucleus pulposus cells into a construct composed of collagen II as well as hyaluronan and chondroitin-6-sulfate, which they implanted into rabbit nucleus pulposus. They noted survival of the seeded cells as well as improved disc space narrowing and T2-weighted MRI signal as compared with study controls [112]. Injectable collagen gels have been developed and been successfully seeded with ovine cells. The collagen was also able to be oriented in a lamellar manner.

Tissue engineering strategies have also been implemented to restore the integrity of the annulus fibrosus, rather than solely trying to restore its tissue component. Patches and biocompatible barriers have been developed which seek to prevent further nucleus pulposus extrusion through tears in the annulus fibrosus. A polyglycolic acid patch was microsurgically sutured to the annulus fibrosus wall defect and led to sealing in of the nucleus pulposus in a canine cadaveric model [114–116]. Other synthetic materials, such as lactide and trimethylene carbonate, have been used to create patches as well, which can be inserted through the annulus fibrosus defect and sewn onto the inner wall. Sharifi *et al.* demonstrated a photopolymerized poly(D,L-lactide-co-trimethylene carbonate) network which mimicked the mechanical properties of human annulus fibrosus and promoted cell adhesion and proliferation *in vitro* [117]. Adhesive glue derived from cyanoacrylate, fibrin-based sealants, and other compounds have also been used in conjunction with sutures to control the defects in the annulus fibrosus [118–125]. These have been used in preclinical studies to seal annu-

lus fibrosus defects and also to prevent further tearing of small annulus fibrosus fissures. Previous attempts have been faulted for their toxicity to the surrounding matrix, or their rigidity, or their suboptimal geometries [126]. Sealing in the defects may also not eliminate the back pain produced by the initial herniation. Future studies will continue to investigate these measures to optimize engineered methods to be implemented in human trials.

Conclusion & future perspective

For many years, the gold standard of care for promoting bony fusion has been autograft, but due to significant complications and limited availability of donor tissue, alternatives are needed. Bone allografts met this need, but their limitations and small risk of infection create a demand for tissue-engineered devices. Nanoscale production techniques such as TIPS, electrospinning and SFF/3D printing will continue to improve allowing more precise control over the 3D microstructure of tissue-engineered constructs. Ongoing research will elucidate how these engineered devices can be combined with biologics including stem cells, growth factors and cytokines to optimize bone and soft tissue regeneration in the spine.

The field of tissue engineering has advanced rapidly in recent years and produced a wide array of materials and constructs for use in bone healing and disc repair and regeneration. There is no single formula to create an ideal tissue-engineered scaffold because different sites of injury require a different environment for optimal healing. As the field of tissue engineering continues to advance and biomimetic scaffolds transition from the pre-clinical phase to clinical trials, the reality of having tissue-engineered solutions draws nearer.

Financial & competing interests disclosure

The authors have no relevant affiliations or financial involvement with any organization or entity with a financial interest in or financial conflict with the subject matter or materials discussed in the manuscript. This includes employment, consultancies, honoraria, stock ownership or options, expert testimony, grants or patents received or pending, or royalties.

No writing assistance was utilized in the production of this manuscript.

Executive summary

Bone graft substitutes

- Demineralized bone matrix, ceramics, cements, glass and mineralized collagen have been investigated as alternatives to bone autograft and allograft for use in osteosynthesis applications.

Biomimetic 3D scaffolds

- Tissue engineering techniques such as electrospinning, thermally induced phase separation and 3D printing have allowed development of customizable biomimetic scaffolds.
- Scaffolds can combine synthetic substrates with stem cells, growth factors and/or cytokines to facilitate bone regeneration.

Bone morphogenetic protein

- Bone morphogenetic protein has gained widespread acceptance, is available through a variety of vehicles, and is used in many aspects of spine surgery.
- However, recent research has identified potential risks and complications associated with its use.

Mesenchymal stem cells

- Still in its infancy, the applications for mesenchymal stem cells in spine surgery are a booming research topic though data to support its efficacy are limited at this point.

Intervertebral disc regeneration

- Disc arthroplasty has shown promising results at 2-year follow-up and is US FDA approved for single level procedures.
- Regenerative strategies including chondrocyte transplantation, scaffolds, growth factors and cytokines are under investigation though preclinical and early clinical data are mixed.
- Strategies for regenerating both the nucleus pulposus and the annulus fibrosus have shown promise in preclinical testing.

References

Papers of special note have been highlighted as:
• of interest

1 Marino JT, Ziran BH. Use of solid and cancellous autologous bone graft for fractures and nonunions. *Orthop. Clin. North Am.* 41(1), 15 –26 (2010).

2 Delloye C, Cornu O, Druez V, Barbier O. Bone allografts: what they can offer and what they cannot. *J. Bone Joint Surg. Br.* 89(5), 574–579 (2007).

3 Younger EM, Chapman MW. Morbidity at bone graft donor sites. *J. Orthop. Trauma* 3(3), 192–195 (1989).

4 Ahlmann E, Patzakis M, Roidis N, Shepherd L, Holtom P. Comparison of anterior and posterior iliac crest bone grafts in terms of harvest-site morbidity and functional outcomes. *J. Bone Joint Surg. Am.* 84-A(5), 716–720 (2002).

5 Dimitriou R, Mataliotakis GI, Angoules AG, Kanakaris NK, Giannoudis PV. Complications following autologous bone graft harvesting from the iliac crest and using the

RIA: a systematic review. *Injury* 42(Suppl. 2), S3–S15 (2011).

6 De Long WG Jr, Einhorn TA, Koval K *et al.* Bone grafts and bone graft substitutes in orthopaedic trauma surgery. A critical analysis. *J. Bone Joint Surg. Am.* 89(3), 649–658 (2007).

• **Excellent review of the evidence for bone graft substitutes.**

7 Grover V, Kapoor A, Malhotra R, Sachdeva S. Bone allografts: a review of safety and efficacy. *Indian J. Dent. Res.* 22(3), 496 (2011).

8 Greenwald AS, Boden SD, Goldberg VM, Khan Y, Laurencin CT, Rosier RN. Bone-graft substitutes: facts, fictions, and applications. *J. Bone Joint Surg. Am.* 83-A(Suppl. 2), Pt 2, 98–103 (2001).

9 Harris JS, Bemenderfer TB, Wessel AR, Kacena MA. A review of mouse critical size defect models in weight bearing bones. *Bone* 55(1), 241–247 (2013).

10 Yoshikawa H, Myoui A. Bone tissue engineering with porous hydroxyapatite ceramics. *J. Artif. Organs* 8(3), 131–136 (2005).

11 Giannoudis PV, Dinopoulos H, Tsiridis E. Bone substitutes: an update. *Injury* 36(Suppl. 3), S20–S27 (2005).

• **Good overview of general principles of bone graft substitutes and different classes of materials used.**

12 Kaiser MG, Groff MW, Watters WC 3rd *et al.* Guideline update for the performance of fusion procedures for degenerative disease of the lumbar spine. Part 16: bone graft extenders and substitutes as an adjunct for lumbar fusion. *J. Neurosurg. Spine* 21(1), 106–132 (2014).

13 Baumann F, Krutsch W, Pfeifer C, Neumann C, Nerlich M, Loibl M. Posterolateral fusion in acute traumatic thoracolumbar fractures: a comparison of demineralized bone matrix and autologous bone graft. *Acta Chir. Orthop. Traumatol. Cech.* 82(2), 119–125 (2015).

14 Ajiboye RM, Hamamoto JT, Eckardt MA, Wang JC. Clinical and radiographic outcomes of concentrated bone marrow aspirate with allograft and demineralized bone matrix for posterolateral and interbody lumbar fusion in elderly patients. *Eur. Spine J.* doi:10.1007/s00586-015-4117-5 (2015) (Epub ahead of print).

15 Zimmermann G, Moghaddam A. Allograft bone matrix versus synthetic bone graft substitutes. *Injury* 42(Suppl. 2), S16–S21 (2011).

16 Pilliar RM, Filiaggi MJ, Wells JD, Grynpas MD, Kandel RA. Porous calcium polyphosphate scaffolds for bone substitute applications – *in vitro* characterization. *Biomaterials* 22(9), 963–972 (2001).

17 Rizzi SC, Heath DJ, Coombes AG, Bock N, Textor M, Downes S. Biodegradable polymer/hydroxyapatite composites: surface analysis and initial attachment of human osteoblasts. *J. Biomed. Mater. Res.* 55(4), 475–486 (2001).

18 Murphy CM, O'brien FJ, Little DG, Schindeler A. Cell-scaffold interactions in the bone tissue engineering triad. *Eur. Cell Mater.* 26, 120–132 (2013).

19 Frankenburg EP, Goldstein SA, Bauer TW, Harris SA, Poser RD. Biomechanical and histological evaluation of a calcium phosphate cement. *J. Bone Joint Surg. Am.* 80A(8), 1112–1124 (1998).

20 Ikenaga M, Hardouin P, Lemaitre J, Andrianjatovo H, Flautre B. Biomechanical characterization of a biodegradable calcium phosphate hydraulic cement: a comparison with porous biphasic calcium phosphate ceramics. *J. Biomed. Mater. Res.* 40(1), 139–144 (1998).

21 Korovessis P, Koureas G, Zacharatos S, Papazisis Z, Lambiris E. Correlative radiological, self-assessment and clinical analysis of evolution in instrumented dorsal and lateral fusion for degenerative lumbar spine disease. Autograft versus coralline hydroxyapatite. *Eur. Spine J.* 14(7), 630–638 (2005).

22 Lee JH, Hwang CJ, Song BW, Koo KH, Chang BS, Lee CK. A prospective consecutive study of instrumented posterolateral lumbar fusion using synthetic hydroxyapatite (Bongros-HA) as a bone graft extender. *J. Biomed. Mater. Res. A* 90(3), 804–810 (2009).

23 Ziran BH, Smith WR, Morgan SJ. Use of calcium-based demineralized bone matrix/allograft for nonunions and posttraumatic reconstruction of the appendicular skeleton: preliminary results and complications. *J. Trauma* 63(6), 1324–1328 (2007).

24 Chen WJ, Tsai TT, Chen LH *et al.* The fusion rate of calcium sulfate with local autograft bone compared with autologous iliac bone graft for instrumented short-segment spinal fusion. *Spine (Phila Pa 1976)* 30(20), 2293–2297 (2005).

25 Dai LY, Jiang LS. Single-level instrumented posterolateral fusion of lumbar spine with beta-tricalcium phosphate versus autograft: a prospective, randomized study with 3-year follow-up. *Spine (Phila Pa 1976)* 33(12), 1299–1304 (2008).

• **Excellent prospective, randomized trial with 3-year follow-up examining beta tri-calcium phosphate as a bone graft substitute in lumbar fusion.**

26 Nishikawa M, Myoui A, Ohgushi H, Ikeuchi M, Tamai N, Yoshikawa H. Bone tissue engineering using novel interconnected porous hydroxyapatite ceramics combined with marrow mesenchymal cells: quantitative and three-dimensional image analysis. *Cell Transplant.* 13(4), 367–376 (2004).

27 Yoshikawa H, Tamai N, Murase T, Myoui A. Interconnected porous hydroxyapatite ceramics for bone tissue engineering. *J. R. Soc. Interface* 6(Suppl. 3), S341–S348 (2009).

28 Hench LL, Splinter RJ, Allen WC, Greenlee TK. Bonding mechanisms at the interface of ceramic prosthetic materials. *J. Biomed. Mater. Res.* 5(6), 117–141 (1971).

29 Blaker JJ, Maquet V, Jerome R, Boccaccini AR, Nazhat SN. Mechanical properties of highly porous PDLLA/Bioglass composite foams as scaffolds for bone tissue engineering. *Acta Biomater.* 1(6), 643–652 (2005).

30 Maquet V, Boccaccini AR, Pravata L, Notingher I, Jerome R. Porous poly(alpha-hydroxyacid)/Bioglass composite scaffolds for bone tissue engineering. I: preparation and *in vitro* characterisation. *Biomaterials* 25(18), 4185–4194 (2004).

31 Yunos DM, Ahmad Z, Boccaccini AR. Fabrication and characterization of electrospun poly-DL-lactide (PDLLA) fibrous coatings on 45S5 Bioglass® substrates for bone tissue engineering applications. *J. Chem. Technol. Biotechnol.* 85(6), 768–774 (2010).

32 Xu C, Su P, Chen X *et al.* Biocompatibility and osteogenesis of biomimetic Bioglass–Collagen–Phosphatidylserine composite scaffolds for bone tissue engineering. *Biomaterials* 32(4), 1051–1058 (2011).

33 Lee JH, Ryu HS, Seo JH, Lee DY, Chang BS, Lee CK. Negative effect of rapidly resorbing properties of bioactive glass-ceramics as bone graft substitute in a rabbit lumbar fusion model. *Clin. Orthop. Surg.* 6(1), 87–95 (2014).

34 Yokoyama Y, Hattori S, Yoshikawa C *et al.* Novel wet electrospinning system for fabrication of spongiform nanofiber 3-dimensional fabric. *Mater. Lett.* 63(9–10), 754–756 (2009).

35 Badami AS, Kreke MR, Thompson MS, Riffle JS, Goldstein AS. Effect of fiber diameter on spreading, proliferation, and differentiation of osteoblastic cells on electrospun poly(lactic acid) substrates. *Biomaterials* 27(4), 596–606 (2006).

36 Boland ED, Telemeco TA, Simpson DG, Wnek GE, Bowlin GL. Utilizing acid pretreatment and electrospinning to improve biocompatibility of poly(glycolic acid) for tissue engineering. *J. Biomed. Mater. Res. B Appl. Biomater.* 71(1), 144–152 (2004).

37 Lee SJ, Oh SH, Liu J, Soker S, Atala A, Yoo JJ. The use of thermal treatments to enhance the mechanical properties of electrospun poly(epsilon-caprolactone) scaffolds. *Biomaterials* 29(10), 1422–1430 (2008).

38 Luo CJ, Nangrejo M, Edirisinghe M. A novel method of selecting solvents for polymer electrospinning. *Polymer* 51(7), 1654–1662 (2010).

39 Zeng J, Aigner A, Czubayko F, Kissel T, Wendorff JH, Greiner A. Poly(vinyl alcohol) nanofibers by electrospinning as a protein delivery system and the retardation of enzyme release by additional polymer coatings. *Biomacromolecules* 6(3), 1484–1488 (2005).

40 Zhang Y, Ouyang H, Lim CT, Ramakrishna S, Huang ZM. Electrospinning of gelatin fibers and gelatin/PCL composite fibrous scaffolds. *J. Biomed. Mater. Res. B Appl. Biomater.* 72(1), 156–165 (2005).

41 Smith LA, Ma PX. Computer-designed nano-fibrous scaffolds. *Methods Mol. Biol.* 868, 125–134 (2012).

42 Ma PX, Zhang R. Synthetic nano-scale fibrous extracellular matrix. *J. Biomed. Mater. Res.* 46(1), 60–72 (1999).

43 Lu L, Zhang Q, Wootton D *et al.* Biocompatibility and biodegradation studies of PCL/beta-TCP bone tissue scaffold fabricated by structural porogen method. *J. Mater. Sci. Mater. Med.* 23(9), 2217–2226 (2012).

44 Lu L, Zhang Q, Wootton DM *et al.* Mechanical study of polycaprolactone-hydroxyapatite porous scaffolds created by porogen-based solid freeform fabrication method. *J. Appl. Biomater. Funct. Mater.* 12(3), 145–154 (2014).

45 Wei G, Ma PX. Macroporous and nanofibrous polymer scaffolds and polymer/bone-like apatite composite scaffolds generated by sugar spheres. *J. Biomed. Mater. Res. A* 78(2), 306–315 (2006).

46 Chen VJ, Smith LA, Ma PX. Bone regeneration on computer-designed nano-fibrous scaffolds. *Biomaterials* 27(21), 3973–3979 (2006).

47 Faundez AA, Taylor S, Kaelin AJ. Instrumented fusion of thoracolumbar fracture with type I mineralized collagen matrix combined with autogenous bone marrow as a bone graft substitute: a four-case report. *Eur. Spine J.* 15(Suppl. 5), 630–635 (2006).

48 Lian K, Lu H, Guo X, Cui F, Qiu Z, Xu S. The mineralized collagen for the reconstruction of intra-articular calcaneal fractures with trabecular defects. *Biomatter.* 3(4), e27250 (2013).

49 Khoueir P, Oh BC, Dirisio DJ, Wang MY. Multilevel anterior cervical fusion using a collagen-hydroxyapatite matrix with iliac crest bone marrow aspirate: an 18-month follow-up study. *Neurosurgery* 61(5), 963–970 (2007).

50 Yu XEA. Clinical evaluation of mineralized collagen as a bone graft substitute for anterior cervical intersomatic fusion. *J. Biomater. Tissue Eng.* 2(2), 170–176 (2012).

51 Shield FBCB. Medical Coverage Guidelines (2014). http://mcgs.bcbsfl.com/

52 Mckay WF, Peckham SM, Badura JM. A comprehensive clinical review of recombinant human bone morphogenetic protein-2 (INFUSE Bone Graft). *Int. Orthop.* 31(6), 729–734 (2007).

53 Fu R, Selph S, Mcdonagh M *et al.* Effectiveness and harms of recombinant human bone morphogenetic protein-2 in spine fusion: a systematic review and meta-analysis. *Ann. Intern. Med.*158(12), 890–902 (2013).

- **Meta-analysis reviewing safety and effectiveness of bone morphogenetic protein in spine fusion, data on effectiveness.**

54 Simmonds MC, Brown JV, Heirs MK *et al.* Safety and effectiveness of recombinant human bone morphogenetic protein-2 for spinal fusion: a meta-analysis of individual-participant data. *Ann. Intern. Med.* 158(12), 877–889 (2013).

- **Important meta-analysis reviewing safety and effectiveness of bone morphogenetic protein in spine fusion.**

55 Epstein NE. Basic science and spine literature document bone morphogenetic protein increases cancer risk. *Surg. Neurol. Int.* 5(Suppl. 15), S552–S560 (2014).

56 Singh K, Nandyala SV, Marquez-Lara A *et al.* Clinical sequelae after rhBMP-2 use in a minimally invasive transforaminal lumbar interbody fusion. *Spine J.* 13(9), 1118–1125 (2013).

57 Ace Surgical Supply Co. I. Osteocel Plus Product Brochure (2014). www.acesurgical.com/index.php

58 Kerr EJ, 3rd, Jawahar A, Wooten T, Kay S, Cavanaugh DA, Nunley PD. The use of osteo-conductive stem-cells allograft in lumbar interbody fusion procedures: an alternative to recombinant human bone morphogenetic protein. *J. Surg. Orthop. Adv.* 20(3), 193–197 (2011).

59 Ammerman JM, Libricz J, Ammerman MD. The role of Osteocel Plus as a fusion substrate in minimally invasive instrumented transforaminal lumbar interbody fusion. *Clin. Neurol. Neurosurg.* 115(7), 991–994 (2013).

60 Bertagnoli R, Yue JJ, Shah RV *et al.* The treatment of disabling single-level lumbar discogenic low back pain with total disc arthroplasty utilizing the Prodisc prosthesis: a prospective study with 2-year minimum follow-up. *Spine (Phila Pa 1976)* 30(19), 2230–2236 (2005).

- **Good prospective study showing 2-year follow-up data for disc arthroplasty in single level.**

61 Blumenthal S, Mcafee PC, Guyer RD *et al.* A prospective, randomized, multicenter Food and Drug Administration investigational device exemptions study of lumbar total disc replacement with the CHARITE artificial disc versus lumbar fusion: part I: evaluation of clinical outcomes. *Spine (Phila Pa 1976)* 30(14), 1565–1575 (2005).

62 Mcafee PC, Cunningham B, Holsapple G *et al.* A prospective, randomized, multicenter Food and Drug Administration investigational device exemption study of lumbar total disc replacement with the CHARITE artificial disc versus lumbar fusion: part II: evaluation of radiographic outcomes and correlation of surgical technique accuracy with clinical outcomes. *Spine (Phila Pa 1976)* 30(14), 1576–1583 (2005).

63 Zeegers WS, Bohnen LM, Laaper M, Verhaegen MJ. Artificial disc replacement with the modular type SB Charite III: 2-year results in 50 prospectively studied patients. *Eur. Spine J.* 8(3), 210–217 (1999).

64 Zigler JE. Clinical results with ProDisc: European experience and U.S. investigation device exemption study. *Spine (Phila Pa 1976)* 28(20), S163–166 (2003).

65 Zigler J, Delamarter R, Spivak JM *et al.* Results of the prospective, randomized, multicenter Food and Drug Administration investigational device exemption study of the ProDisc-L total disc replacement versus circumferential fusion for the treatment of 1-level degenerative disc disease. *Spine (Phila Pa 1976)* 32(11), 1155–1162 (2007).

66 Yao Q, Liang F, Xia Y, Jia C. A meta-analysis comparing total disc arthroplasty with anterior cervical discectomy and fusion for the treatment of cervical degenerative diseases. *Arch. Orthop. Trauma Surg.* doi:10.1007/s00402-015-2337-0 (2015) (Epub ahead of print).

67 Meisel HJ, Ganey T, Hutton WC, Libera J, Minkus Y, Alasevic O. Clinical experience in cell-based therapeutics: intervention and outcome. *Eur. Spine J.* 15(Suppl. 3), S397–S405 (2006).

68 Meisel HJ, Siodla V, Ganey T, Minkus Y, Hutton WC, Alasevic OJ. Clinical experience in cell-based therapeutics: disc chondrocyte transplantation A treatment for degenerated or damaged intervertebral disc. *Biomol. Eng.* 24(1), 5–21 (2007).

69 Hohaus C, Ganey TM, Minkus Y, Meisel HJ. Cell transplantation in lumbar spine disc degeneration disease. *Eur. Spine J.* 17(Suppl. 4), 492–503 (2008).

70 O'halloran DM, Pandit AS. Tissue-engineering approach to regenerating the intervertebral disc. *Tissue Eng.* 13(8), 1927–1954 (2007).

71 Yang X, Li X. Nucleus pulposus tissue engineering: a brief review. *Eur. Spine J.* 18(11), 1564–1572 (2009).

72 Chujo T, An HS, Akeda K *et al.* Effects of growth differentiation factor-5 on the intervertebral disc – *in vitro* bovine study and *in vivo* rabbit disc degeneration model study. *Spine (Phila Pa 1976)* 31(25), 2909–2917 (2006).

73 Cui M, Wan Y, Anderson DG *et al.* Mouse growth and differentiation factor-5 protein and DNA therapy potentiates intervertebral disc cell aggregation and chondrogenic gene expression. *Spine J.* 8(2), 287–295 (2008).

74 Walsh AJ, Bradford DS, Lotz JC. *In vivo* growth factor treatment of degenerated intervertebral discs. *Spine (Phila Pa 1976)* 29(2), 156–163 (2004).

75 Chan S, Gantenbein-Ritter B. Intervertebral disc regeneration or repair with biomaterials and stem cell therapy – feasible or fiction? *Swiss Med. Wkly* 142, w13598 (2012).

76 Depuy-Spine. Intradiscal rhGDF-5 Phase I/II clinical trial. https://clinicaltrials.gov/ct2/show/NCT00813813

77 Li X, Lee JP, Balian G, Greg Anderson D. Modulation of chondrocytic properties of fat-derived mesenchymal cells in co-cultures with nucleus pulposus. *Connect. Tissue Res.* 46(2), 75–82 (2005).

78 Lu ZF, Zandieh Doulabi B, Wuisman PI, Bank RA, Helder MN. Differentiation of adipose stem cells by nucleus pulposus cells: configuration effect. *Biochem. Biophys. Res. Commun.* 359(4), 991–996 (2007).

79 Tapp H, Deepe R, Ingram JA, Kuremsky M, Hanley EN Jr, Gruber HE. Adipose-derived mesenchymal stem cells from the sand rat: transforming growth factor beta and 3D co-culture with human disc cells stimulate proteoglycan and collagen type I rich extracellular matrix. *Arthritis Res. Ther.* 10(4), R89 (2008).

80 Feng G, Wan Y, Balian G, Laurencin CT, Li X. Adenovirus-mediated expression of growth and differentiation factor-5 promotes chondrogenesis of adipose stem cells. *Growth Factors* 26(3), 132–142 (2008).

81 Sun W, Zhang K, Liu G *et al.* Sox9 gene transfer enhanced regenerative effect of bone marrow mesenchymal stem cells on the degenerated intervertebral disc in a rabbit model. *PLoS ONE* 9(4), e93570 (2014).

82 Nomura T, Mochida J, Okuma M, Nishimura K, Sakabe K. Nucleus pulposus allograft retards intervertebral disc degeneration. *Clin. Orthop. Relat. Res.* (389), 94–101 (2001).

83 Boyd LM, Carter AJ. Injectable biomaterials and vertebral endplate treatment for repair and regeneration of the intervertebral disc. *Eur. Spine J.* 15(Suppl. 3), S414–S421 (2006).

84 Chou AI, Nicoll SB. Characterization of photocrosslinked alginate hydrogels for nucleus pulposus cell encapsulation. *J. Biomed. Mater. Res. A* 91(1), 187–194 (2009).

85 Cho J, Heuzey MC, Begin A, Carreau PJ. Physical gelation of chitosan in the presence of beta-glycerophosphate: the effect of temperature. *Biomacromolecules* 6(6), 3267–3275 (2005).

86 Di Martino A, Sittinger M, Risbud MV. Chitosan: a versatile biopolymer for orthopaedic tissue-engineering. *Biomaterials* 26(30), 5983–5990 (2005).

87 Nair LS, Starnes T, Ko JW, Laurencin CT. Development of injectable thermogelling chitosan-inorganic phosphate solutions for biomedical applications. *Biomacromolecules* 8(12), 3779–3785 (2007).

88 Bader RA, Rochefort WE. Rheological characterization of photopolymerized poly(vinyl alcohol) hydrogels for potential use in nucleus pulposus replacement. *J. Biomed. Mater. Res. A* 86(2), 494–501 (2008).

89 Richardson SM, Hughes N, Hunt JA, Freemont AJ, Hoyland JA. Human mesenchymal stem cell differentiation to NP-like cells in chitosan-glycerophosphate hydrogels. *Biomaterials* 29(1), 85–93 (2008).

90 Roughley P, Hoemann C, Desrosiers E, Mwale F, Antoniou J, Alini M. The potential of chitosan-based gels containing intervertebral disc cells for nucleus pulposus supplementation. *Biomaterials* 27(3), 388–396 (2006).

91 Joung YK, Bae JW, Park KD. Controlled release of heparin-binding growth factors using heparin-containing particulate systems for tissue regeneration. *Expert Opin. Drug Deliv.* 5(11), 1173–1184 (2008).

92 Li J, Zhu B, Shao Y, Liu X, Yang X, Yu Q. Construction of anticoagulant poly (lactic acid) films via surface covalent graft of heparin-carrying microcapsules. *Colloids Surf. B Biointerfaces* 70(1), 15–19 (2009).

93 Murugesan S, Xie J, Linhardt RJ. Immobilization of heparin: approaches and applications. *Curr. Top. Med. Chem.* 8(2), 80–100 (2008).

94 Edlund U, Danmark S, Albertsson AC. A strategy for the covalent functionalization of resorbable polymers with heparin and osteoinductive growth factor. *Biomacromolecules* 9(3), 901–905 (2008).

95 Fujita M, Ishihara M, Simizu M *et al.* Vascularization *in vivo* caused by the controlled release of fibroblast growth factor-2 from an injectable chitosan/non-anticoagulant heparin hydrogel. *Biomaterials* 25(4), 699–706 (2004).

96 Gruber HE, Norton HJ, Hanley EN Jr. Anti-apoptotic effects of IGF-1 and PDGF on human intervertebral disc cells *in vitro*. *Spine (Phila Pa 1976)* 25(17), 2153–2157 (2000).

97 Saal JA, Saal JS. Intradiscal electrothermal treatment for chronic discogenic low back pain: a prospective outcome study with minimum 1-year follow-up. *Spine (Phila Pa 1976)* 25(20), 2622–2627 (2000).

98 Emans PJ, Pieper J, Hulsbosch MM *et al.* Differential cell viability of chondrocytes and progenitor cells in tissue-engineered constructs following implantation into osteochondral defects. *Tissue Eng.* 12(6), 1699–1709 (2006).

99 Ma T, Grayson WL, Frohlich M, Vunjak-Novakovic G. Hypoxia and stem cell-based engineering of mesenchymal tissues. *Biotechnol. Prog.* 25(1), 32–42 (2009).

100 Moioli EK, Clark PA, Chen M *et al.* Synergistic actions of hematopoietic and mesenchymal stem/progenitor cells in vascularizing bioengineered tissues. *PLoS ONE* 3(12), e3922 (2008).

101 Potier E, Ferreira E, Meunier A, Sedel L, Logeart-Avramoglou D, Petite H. Prolonged hypoxia concomitant with serum deprivation induces massive human mesenchymal stem cell death. *Tissue Eng.* 13(6), 1325–1331 (2007).

102 Reza AT, Nicoll SB. Hydrostatic pressure differentially regulates outer and inner annulus fibrosus cell matrix production in 3D scaffolds. *Ann. Biomed. Eng.* 36(2), 204–213 (2008).

103 Moran JM, Pazzano D, Bonassar LJ. Characterization of polylactic acid-polyglycolic acid composites for cartilage tissue engineering. *Tissue Eng.* 9(1), 63–70 (2003).

104 Mizuno H, Roy AK, Vacanti CA, Kojima K, Ueda M, Bonassar LJ. Tissue-engineered composites of anulus fibrosus and nucleus pulposus for intervertebral disc replacement. *Spine (Phila Pa 1976)* 29(12), 1290–1297(2004).

105 Mizuno H, Roy AK, Zaporojan V, Vacanti CA, Ueda M, Bonassar LJ. Biomechanical and biochemical characterization of composite tissue-engineered intervertebral discs. *Biomaterials* 27(3), 362–370 (2006).

106 Nerurkar NL, Baker BM, Sen S, Wible EE, Elliott DM, Mauck RL. Nanofibrous biologic laminates replicate the form and function of the annulus fibrosus. *Nat. Mater.* 8(12), 986–992 (2009).

107 Nerurkar NL, Elliott DM, Mauck RL. Mechanics of oriented electrospun nanofibrous scaffolds for annulus fibrosus tissue engineering. *J. Orthop. Res.* 25(8), 1018–1028 (2007).

108 Nerurkar NL, Mauck RL, Elliott DM. ISSLS prize winner: integrating theoretical and experimental methods for functional tissue engineering of the annulus fibrosus. *Spine (Phila Pa 1976)* 33(25), 2691–2701 (2008).

109 Chang G, Kim HJ, Kaplan D, Vunjak-Novakovic G, Kandel RA. Porous silk scaffolds can be used for tissue engineering annulus fibrosus. *Eur. Spine J.* 16(11), 1848–1857 (2007).

110 Chang G, Kim HJ, Vunjak-Novakovic G, Kaplan DL, Kandel R. Enhancing annulus fibrosus tissue formation in porous silk scaffolds. *J. Biomed. Mater. Res. A* 92(1), 43–51 (2010).

111 Bowles RD, Williams RM, Zipfel WR, Bonassar LJ. Self-assembly of aligned tissue-engineered annulus fibrosus and intervertebral disc composite via collagen gel contraction. *Tissue Eng. Part A* 16(4), 1339–1348 (2010).

112 Huang B, Zhuang Y, Li CQ, Liu LT, Zhou Y. Regeneration of the intervertebral disc with nucleus pulposus cell-seeded collagen II/hyaluronan/chondroitin-6-sulfate tri-copolymer constructs in a rabbit disc degeneration model. *Spine (Phila Pa 1976)* 36(26), 2252–2259 (2011).

113 Sato M, Asazuma T, Ishihara M *et al.* An experimental study of the regeneration of the intervertebral disc with an allograft of cultured annulus fibrosus cells using a tissue-engineering method. *Spine (Phila Pa 1976)* 28(6), 548–553 (2003).

114 Abbushi A, Endres M, Cabraja M *et al.* Regeneration of intervertebral disc tissue by resorbable cell-free polyglycolic acid-based implants in a rabbit model of disc degeneration. *Spine (Phila Pa 1976)* 33(14), 1527–1532 (2008).

115 Hegewald AA, Ringe J, Sittinger M, Thome C. Regenerative treatment strategies in spinal surgery. *Front Biosci.* 13, 1507–1525 (2008).

116 Singh V, Piryani C, Liao K, Nieschulz S. Percutaneous disc decompression using coblation (nucleoplasty) in the treatment of chronic discogenic pain. *Pain Physician* 5(3), 250–259 (2002).

117 Sharifi S, Van Kooten TG, Kranenburg HJ *et al.* An annulus fibrosus closure device based on a biodegradable shape-memory polymer network. *Biomaterials* 34(33), 8105–8113 (2013).

118 Heuer F, Ulrich S, Claes L, Wilke HJ. Biomechanical evaluation of conventional anulus fibrosus closure methods required for nucleus replacement. Laboratory investigation. *J. Neurosurg. Spine* 9(3), 307–313 (2008).

119 Chen WL, Lin CT, Hsieh CY, Tu IH, Chen WY, Hu FR. Comparison of the bacteriostatic effects, corneal cytotoxicity, and the ability to seal corneal incisions among three different tissue adhesives. *Cornea* 26(10), 1228–1234 (2007).

120 Schek RM, Michalek AJ, Iatridis JC. Genipin-crosslinked fibrin hydrogels as a potential adhesive to augment intervertebral disc annulus repair. *Eur. Cell Mater.* 21, 373–383 (2011).

121 Wang JC, Alanay A, Mark D *et al.* A comparison of commercially available demineralized bone matrix for spinal fusion. *Eur. Spine J.* 16(8), 1233–1240 (2007).

122 Murakami Y, Yokoyama M, Okano T *et al.* A novel synthetic tissue-adhesive hydrogel using a crosslinkable polymeric micelle. *J. Biomed. Mater. Res. A* 80(2), 421–427 (2007).

123 Sharifi S, Blanquer SB, Van Kooten TG, Grijpma DW. Biodegradable nanocomposite hydrogel structures with enhanced mechanical properties prepared by photo-crosslinking solutions of poly(trimethylene carbonate)-poly(ethylene glycol)-poly(trimethylene carbonate) macromonomers and nanoclay particles. *Acta Biomater.* 8(12), 4233–4243 (2012).

124 Blanquer SB, Sharifi S, Grijpma DW. Development of poly(trimethylene carbonate) network implants for annulus fibrosus tissue engineering. *J. Appl. Biomater. Funct. Mater.* 10(3), 177–184 (2012).

125 Yin W PK, Olan W, Doerzbacher J. Long-term outcomes from a prospective, multicenter investigational device exemption (IDE) pilot study of intradiscal fibrin sealant for the treatment of discogenic pain. *Pain Med.* 12(9), 1446–1447 (2011).

126 Bron JL, Van Der Veen AJ, Helder MN, Van Royen BJ, Smit TH. Biomechanical and *in vivo* evaluation of experimental closure devices of the annulus fibrosus designed for a goat nucleus replacement model. *Eur. Spine J.* 19(8), 1347–1355 (2010).

Enhanced osteogenic differentiation with 3D electrospun nanofibrous scaffolds

Aim: Developing 3D scaffolds mimicking the nanoscale structure of the native extracellular matrix is important in tissue regeneration. In this study, we aimed to demonstrate the novelty of 3D nanofibrous scaffolds and compare their efficiency with 2D nanofibrous scaffolds. **Materials & methods:** The 2D poly(L-lactic acid)/collagen nanofibrous scaffolds were 2D meshes fabricated by the conventional electrospinning technique, whereas the 3D poly(L-lactic acid)/collagen nanofibrous scaffolds were fabricated by a modified electrospinning technique using a dynamic liquid support system. The morphology, proliferation and differentiation abilities of human mesenchymal stem cells in osteogenic medium on both scaffolds were investigated. **Results & conclusion:** Compared with the 2D scaffolds, the 3D scaffolds significantly increased the expression of osteoblastic genes of the stem cells as well as the formation of bone minerals. In addition, the scanning electron microscopic and micro-computed tomographic images showed the dense deposition of bone minerals aligned along the nanofibers of the 3D scaffolds after 14 and 28 days cultured with the mesenchymal stem cells. As such, the 3D electrospun poly(L-lactic acid)/collagen nanofibrous scaffold is a novel bone graft substitute for bone tissue regeneration.

Original submitted 17 November 2011; Revised submitted 21 February 2012; Published online 18 June 2012

KEYWORDS: 3D ■ bone ■ collagen ■ nanofiber ■ osteogenic differentiation ■ poly(L-lactic acid)

Luong TH Nguyen*[1], Susan Liao[2], Casey K Chan[3,4] & Seeram Ramakrishna[4,5]

[1]NUS Graduate School for Integrative Sciences & Engineering, National University of Singapore, 28 Medical Drive, 117456, Singapore
[2]School of Materials Science & Engineering, Nanyang Technological University, 50 Nanyang Avenue, 639798, Singapore
[3]Department of Orthopedic Surgery, National University Health System, 1E Kent Ridge Road, 119228, Singapore
[4]National University of Singapore, 9 Engineering Drive 1, 117576, Singapore
[5]King Saud University, Riyadh 11451, Kingdom of Saudi Arabia
**Author for correspondence:*
Tel.: +65 6516 6593
Fax: +65 6773 0339
hienluong@nus.edu.sg

Up to now, most studies on cellular characteristics, such as morphology, adhesion, migration, proliferation and differentiation, have been performed on 2D flat substrates because of the ease and convenience in handling, analyzing and observing them under microscopes, as well as the high cell viability obtained [1,2]. Those 2D flat substrates can be tissue culture flasks, petri dishes, microwell plates or other 2D materials. 2D cell culture systems have notably provided the basic knowledge of cellular biology.

In the body, almost all tissue cells reside in a 3D environment where cell–cell interactions as well as the presentation of chemical, physical, mechanical and electrical stimuli cues in the surrounding fluid and extracellular matrix (ECM) provide the guidance for cellular responses. Owing to the lack of structural cues in 2D culture systems, cells have been forced to adapt to flat and rigid surfaces. This drawback can cause alterations in morphology, metabolism, gene expression patterns and cellular signaling, which may reduce cellular functions [2–5]. As such, 2D substrates are significantly limited in reproducing the complex environments of the body.

Although epithelial cells cultured on flat substrates can recapitulate multilayer sheets and exhibit differentiated 3D histoarchitecture, most cells require cues from truly 3D matrices to create 3D tissue models *in vitro* [6]. Hence, the development of 3D scaffolds play a key role in studying and regulating cellular characteristics. Advances in material chemistry and processing technologies have offered a wide range of 3D scaffolds such as cell entrapping hydrogels, porous scaffolds and scaffolds based on computer assistance [2]. The advantages of 3D scaffolds over 2D scaffolds in cell culture were shown in previous studies. Endothelial cells cultured on plastic or collagen surfaces performed a flattened morphology with a hemispherical cell body; meanwhile the cells cultured inside 3D collagen gels were characterized by a dendritic morphology with a round or spindle-shaped cell body [1]. 3D polyethylene glycol (PEG)-based hydrogels also assisted murine embryonic stem cells with the maintenance of their spherical cellular morphologies [7]. Stem cells cultured in 3D scaffolds such as fibrin and PEGylated fibrin gels [8], self-assembled peptide–amphiphile nanofibrous matrix [9,10], porous polyethylene terephthalate matrix [11,12] and others, had higher proliferation than those on tissue culture plates (TCP). Xie *et al.* indicated that although human mesenchymal stem cells (hMSCs) on 2D surfaces (TCP) had

Future Medicine part of fsg

a higher initial rate, they stopped their proliferation as confluence was reached (~ on day 15) [11]. Meanwhile, the cells in the porous polyethylene terephthalate matrix grew at a stable and lower rate, but lasted for a longer time and achieved a higher final cell number.

In addition to affecting cell morphology and proliferation, 3D scaffolds have been shown to support stem cells to increase differentiation potentials more than 2D scaffolds. Many 3D scaffolds enhanced the hepatocyte differentiation of stem cells (MSCs or embryonic stem cells [ESCs]) such as collagen-coated poly(lactic-*co*-glycolic acid) (PLGA) scaffolds over TCP [13], nonwoven polyethylene terephthalate microfibers over TCP [14], blended poly(L-lactic acid) (PLLA)/PLGA sponges (with or without matrigel) over 2D fibronectin-coated dishes or matrigel alone [15] and collagen sponges over collagen-coated TCP [16,17]. The chondrogenic differentiation of murine ESCs was also improved by 3D PEG-based hydrogels compared with gelatin-coated TCP, in the presence of TGF-β1 [7]. In addition, culturing stem cells in 3D scaffolds increased their osteogenic differentiation ability [9,10,18,19]. MSCs in the self-assembled peptide-amphiphile nanofibrous matrix had higher expressions of osteogenic markers (ALP and OCN) than those on TCP [9,10]. This matrix also significantly promoted the differentiation of ESCs into osteoblast-like cells in comparison with TCP as shown by higher levels of ALP, collagen type I (Col), OPN and calcium phosphate deposits [18]. Moreover, ESCs expressed higher levels of ALP and OCN when cultured in 3D porous PLGA, than on gelatin-coated TCP [19]. After 3 weeks of *in vitro* culture of ESCs in the porous PLGA, the 3D cell-scaffold constructs were implanted in the iliac crests of rabbits, and the new bone formation was detected as early as 4 weeks. Although the above studies have demonstrated the advantages of 3D scaffolds over 2D scaffolds, it is still difficult to confirm whether those advantages are due to another dimension provided by the 3D structures because there have been too many differences in chemical natures, physical structures and initial cell-seeding densities between the 2D and 3D structures.

Collagen nanofibrils account for 95% of the organic matrix of the native bone ECM. Mimicking the nanoscale structure of the ECM plays a significantly important role as an instructive background to guide cell behavior. Among techniques for the fabrication of nanofibrous structures, electrospinning is a highly attractive method owing to its ability to fabricate long continuous strands, to create various nanofibrous architectures as well as its flexibility in the material selection. Recently, the author's group has developed an electrospinning technique for the fabrication of 3D nanofibrous assemblies using a dynamic liquid support system [20,21]. In this study, we focused on the importance of

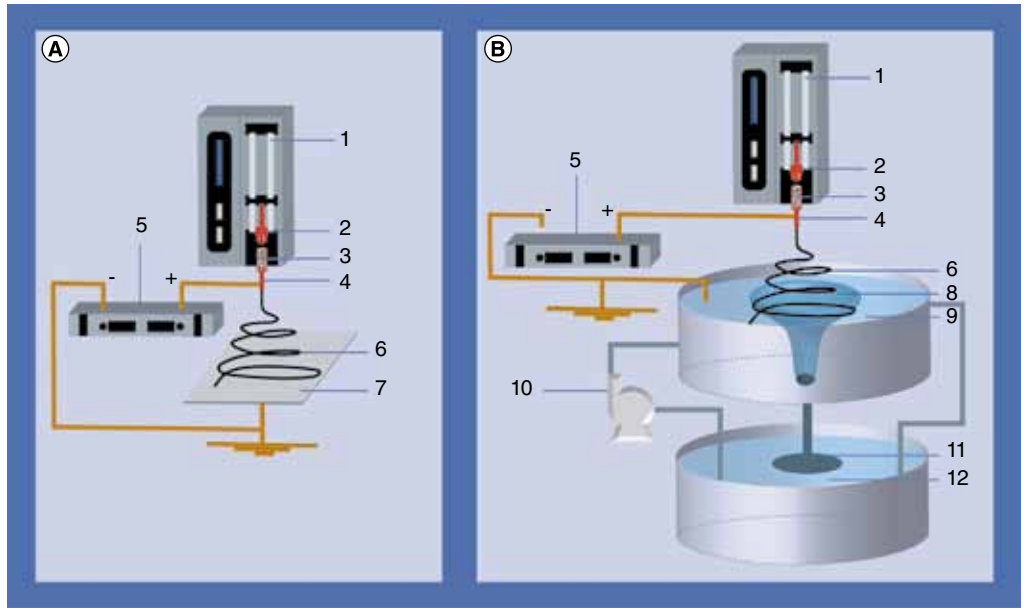

Figure 1. The fabrication of 2D and 3D electrospun poly(L-lactic acid)/collagen type I nanofibrous scaffolds. (A) 2D and **(B)** 3D: (1) syringe pump, (2) syringe, (3) polymer solution, (4) needle, (5) high-voltage power supply, (6) electrospinning jet, (7) metal plate, (8) water vortex, (9) receptacle, (10) dynamic pump, (11) nanofibrous bundles and (12) reservoir.

nanofibrous scaffolds to the osteogenic differentiation ability of hMSCs, which was induced by the presence of osteogenic medium. A comparative study was set up to indicate the role of 3D structures, in which 2D nanofibrous meshes fabricated by the conventional electrospinning technique were used as controls. PLLA and Col were chosen as materials to fabricate the 2D and 3D scaffolds. PLLA has a high mechanical property, suitable for bone tissue regeneration. Meanwhile, collagen is known to support cell adhesion and proliferation [22,23]. The 3D PLLA/Col nanofibrous scaffolds were hypothesized to enhance the osteogenic differentiation of MSCs and support the cells to create a bone ECM-like structure.

Materials & methods

Fabrication of electrospun nanofibers

PLLA (molecular weight 300,000 Da, Polysciences, PA, USA) and Col (Koken, Tokyo, Japan) with the ratio of 80:20 w/w were dissolved in 1,1,1,3,3-hexafluoro-2-propanol (Sigma-Aldrich, MO, USA) to obtain a final concentration of 3% w/v. Figures 1A & B describe the electrospinning techiques to fabricate 2D and 3D nanofibrous scaffolds, respectively. In both techniques, the polymer solution (3) was loaded into a syringe (2) connected with a BD 27G ½ needle (4). The feed rate was kept constantly at 1 ml/h by a KD Scientific syringe pump (1; Holliston, MA, USA). Collectors were placed at a distance of 12 cm from the needle. A high voltage (12 kV) was applied between the needle and the collectors by a direct current high voltage power supply (Gamma High Voltage Research Inc., FL, USA) (5). Electrospinning jets (6) were emitted from the needle and deposited on suitable collectors. For 2D scaffolds, the collector was a metal plate (7) covered by aluminum foil and placed over with 15 mm glass cover slips. After spinning, the scaffolds on the cover slips were vacuum dried overnight to remove any remaining solvent. The average mass of the 2D scaffold (Figure 2A) was 1 mg.

For 3D scaffolds, electrospinning jets were deposited on a receptacle (9) filled with deionized water. When water was drained out from a hole at the bottom of the receptacle, a water vortex (8) was created. Nanofibrous bundles (11) were collected in a reservoir (12) below the receptacle. A dynamic pump (10) was used to circulate water between the receptacle and the reservoir. After spinning, the nanofibrous bundles were placed in a 50 ml centrifuge tube, frozen at 80°C overnight and freeze-dried until they were completely dried. To be applied in cell culture, the 3D scaffold was cut into pieces with the mass of 10 mg (Figure 2B).

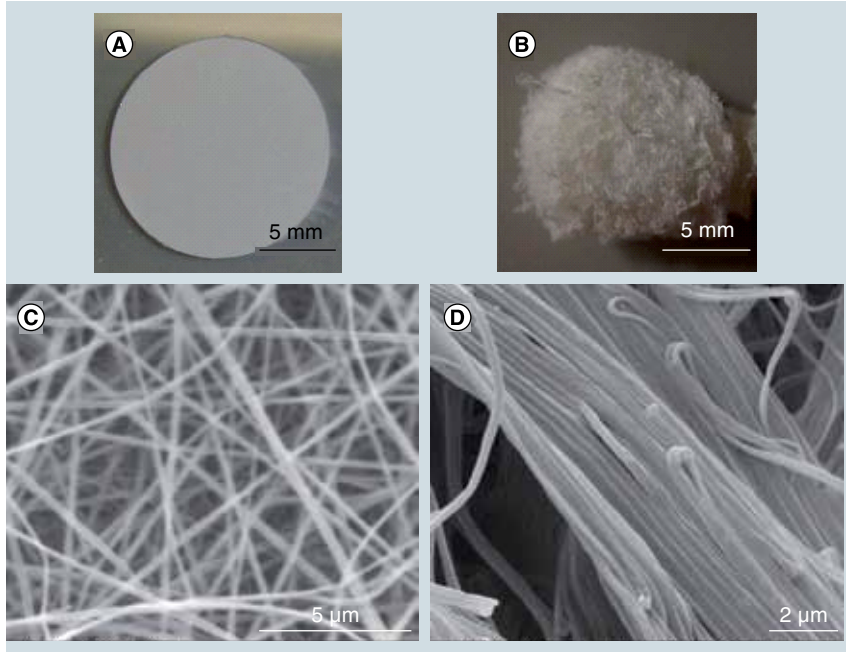

Figure 2. Macroscopic and scanning electron microscopic images of 2D and 3D scaffolds. The macroscopic images of **(A)** 2D and **(B)** 3D scaffolds; and the scanning electron microscopic images of **(C)** 2D and **(D)** 3D scaffolds at 20,000× magnification of electrospun poly(L-lactic acid)/collagen type I nanofibrous scaffolds. Smooth and uniform nanofibers were observed on both types of scaffolds. The average diameters of nanofibers of the 2D and 3D scaffolds were 218.97 ± 66.14 nm and 258.29 ± 70.10 nm, respectively.

Culture of hMSCs

hMSCs (Lonza, MD, USA; passage 2) were cultured in growth medium including α minimum essential medium (α-MEM; Invitrogen, CA, USA), 10% fetal bovine serum (Invitrogen), 100 U/ml penicillin (Sigma-Aldrich) and 100 µg/ml streptomycin (Sigma-Aldrich) in an incubator at 37°C with a humidified atmosphere of 5% CO_2. When the cells reached near confluence (80–90%), they were detached by trypsin/EDTA (Cell Applications, CA, USA) and then subcultured into the next passage.

Osteogenic differentiation of hMSCs

Before seeding with cells, 2D and 3D scaffolds were sterilized under UV light for 30 and 60 min, respectively, and then prewetted in 70% ethanol for 5 min. Subsequently, they were washed three-times with phosphate-buffered saline (PBS; Invitrogen) and once with the growth medium. The scaffolds were then incubated with the growth medium in the incubator for 2 h to facilitate cell attachment.

hMSCs at passage 4 were suspended in the growth medium and seeded on 2D and 3D scaffolds with the density of 10^4 cells/mg scaffold. For the 2D scaffold, cell suspension was directly dropped on the scaffold. For the 3D scaffold, the scaffold was put in a 3-ml syringe, and cell suspension was slowly passed through the syringe for ten-times. The 2D/3D scaffolds and their cell suspension were then incubated together in 24-well plates. After 24 h, all cell-scaffold constructs were changed with osteogenic medium containing the growth medium supplemented with 10 mM β-glycerophosphate (Sigma-Aldrich), 50 μM ascorbate-2-phosphate (Sigma-Aldrich) and 100 nM dexamethasone (Sigma-Aldrich). The medium was then changed every 3 days.

Scanning electron microscopy

After culturing for 3, 14 and 28 days, the cell-scaffold constructs were fixed in 2.5% glutaraldehyde (Sigma-Aldrich) for 1 h, followed by dehydration in sequentially increasing ethanol solutions with 10 min for each concentration (50, 80, 90, 95 and 100%). The samples were subsequently dried in a vacuum overnight. Before observing under a scanning electron microscope (SEM; NOVA™ NanoSEM 230, FEI, OR, USA), the dried samples were gold sputtered with a JFC-1600 Auto Fine Coater (JEOL, Tokyo, Japan) at 10 mA for 90 s (2D scaffolds) or 20 mA for 240 s (3D scaffolds). The mineralized nodules were identified and analyzed by the SEM equipped with an energy dispersive x-ray (EDX) spectrometer. The average diameter of nanofibers was determined from the SEM micrographs using an image analysis software (Image J™, NIH, MD, USA).

Actin cytoskeleton staining

On day 14, the samples were collected and fixed in 4% formaldehyde for 1 h. After washing with PBS, F-actin was stained with tetramethylrhodamine isothiocyanate-conjugated phalloidin (Invitrogen) for 60 min at room temperature. Subsequently, the cell-scaffold constructs were incubated with 4′,6-diamidino-2-phenylindole, dilactate (Invitrogen) for 30 min at room temperature, and then observed under laser scanning confocal microscope (Olympus FluoView® FV1000, Tokyo, Japan).

Cell proliferation

In predetermined time intervals (14, 21 and 28 days), cell proliferation was measured by the Cell-Titer 96® Aqueous One Solution Cell Proliferation Assay (Promega, WI, USA), a colorimetric assay using (3-[4,5-dimethylthiazol-2-yl]-5-[3-carboxymethoxyphenyl]-2-[4-sulfophenyl]-2H-tetrazolium). Briefly, after rinsing culture wells with PBS, the samples were incubated with a reaction solution that was prepared by mixing the CellTiter 96 Aqueous One Solution Reagent and α-MEM at the ratio of 1:5 v/v, for 4 h in the incubator. The absorbance at 490 nm was then recorded using FLUOstar OPTIMA microplate reader (BMG Labtech, Ortenberg, Germany). A calibration curve of hMSCs was established to estimate the number of living cells from the absorbance index.

Real-time reverse transcription-PCR

At determined time points (days 14 and 21), total RNA of the cells in the scaffolds was extracted and purified using RNeasy® Plus Mini Kit (Qiagen, Venlo, The Netherlands). Superscript® III First Strand Synthesis System for reverse transcription-PCR (Invitrogen) was then employed to reverse transcribe the RNA samples into first-strand cDNA using the oligo(dT) method. Real-time PCR was next run with SYBR® Green (Applied Biosystems, CA, USA) using a real-time thermal cycler (iQ™5 Optical System, Bio-Rad, CA, USA). The expression of osteoblastic genes including *ALP*, *OPN*, *OCN* and *WNT5A* were analyzed (Table 1). *GAPDH* was chosen as a housekeeping gene to normalize gene expression using the $\Delta\Delta C_T$ method. PCR reaction conditions were 2 min at 50°C, 10 min at 95°C, and then 45 cycles of 95°C for 15 s and 60°C for 1 min.

Calcium content

After 21 and 28 days, the samples were washed three-times with PBS and extracted calcium

Table 1. Designed primers for real-time PCR.

Gene	Forward primers (5′ 3′)	Reverse primers (5′ 3′)
ALP	CTGATGTGGAGTATGAGAGT	AGTGGGAGTGCTTGTATC
OPN	GTGGGAAGGACAGTTATGA	AATTCACGGCTGACTTTG
OCN	CAGCGAGGTAGTGAAGAG	GATGTGGTCAGCCAACTC
WNT5A	GCCATGAAGAAGTCCATTG	TAGCGACCACCAAGAATT
GAPDH	TGACAACAGCCTCAAGAT	GTCCTTCCACGATACCAA

using 0.5 M acetic acid (Sigma-Aldrich) in an orbital shaker overnight at 37°C. The calcium content in the supernatants was subsequently evaluated by a colorimetric assay using o-cresolphthalein complexone (Calcium Colorimetric Assay Kit, Biovision, CA, USA). Briefly, the supernatants were mixed with the chromogenic reagent and the calcium assay buffer, respectively, and then incubated for 15 min at room temperature. The optical density at 575 nm was finally determined using the microplate reader. The calcium amount was calculated from the calibration curve constructed according to the manufacturer's instructions.

Alizarin red S staining

This staining was utilized to observe the calcium deposition on the ECM on day 28. After rinsing three-times with PBS, the cell-scaffold constructs were fixed in ice-cold 70% ethanol for 1 h at 4°C. The samples were then washed three-times with deionized water and stained with 1.36% Alizarin red S (Sigma-Aldrich) for 1 h at room temperature. They were again washed three-times with deionized water and visualized under light microscope (Leica DC300 F, Wetzlar, Germany).

Micro-computed tomography

The original 3D scaffolds and the 3D cell-scaffold constructs after 14 and 28 days in culture were scanned and reconstructed to create 3D images using phase-contrast imaging and tomography beamline at Singapore Synchrotron Light Source. The energy range of white beam x-ray is about 4–12 keV. The tomography system can acquire images with the pixel size of 6.45 µm.

Statistical analysis

The results given are representative of three independent experiments. Data were analyzed by means of one-factor analysis of variance or multifactor analysis of variance using STATGRAPHICS® Centurion XV (StatPoint Technologies, Inc., VA, USA).

Results

Scaffold morphology

The SEM morphologies of the 2D and 3D scaffolds are shown in Figure 2C & D (with 20,000× magnification) and Supplementary Figure 1 (with 2000× magnification; see online at www.futuremedicine.com/doi/suppl/12.41). Smooth and uniform nanofibers were observed on both types of scaffolds. Because of the difference in fabrication method, there was a difference in the morphologies of the 2D and 3D scaffolds. The 3D scaffold was formed by bundles of curved and coiled nanofibers, while the nanofibers of the 2D scaffold were random and straight. However, there was no significant difference in the fibrous diameters of these scaffolds ($p < 0.05$). The average diameters of the nanofibers of the 2D and 3D scaffolds were 218.97 ± 66.14 nm and 258.29 ± 70.10 nm, respectively.

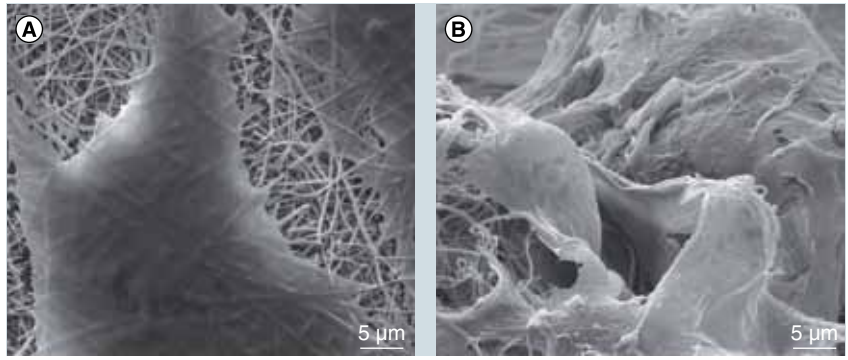

Figure 3. Morphology of human mesenchymal cells on 2D and 3D scaffolds. The morphology of human mesenchymal stem cells cultured on **(A)** 2D and **(B)** 3D electrospun poly(L-lactic acid)/collagen type I nanofibrous scaffolds on day 3. On the 2D scaffolds, the cells were flattened on the surface, while the cells on the 3D scaffolds curved round the scaffold geometry and some of them started to form 3D shapes.

Cell morphology

The morphology of hMSCs after 3 days cultured in the osteogenic medium on both 2D and 3D scaffolds were observed by SEM (Figure 3). The cells attached well and spread on both scaffolds. On the 2D scaffolds, all the cells were flattened on the surface (Figure 3A). Meanwhile, the cells on the 3D scaffolds curved round the scaffold

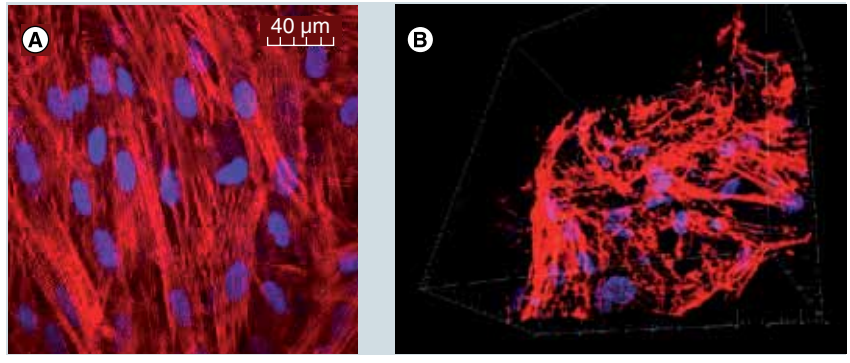

Figure 4. Actin cytoskeleton staining of human mesenchymal stem cells. The actin cytoskeleton staining of human mesenchymal stem cells differentiated in the osteogenic medium on **(A)** 2D and **(B)** 3D electrospun poly(L-lactic acid)/collagen type I nanofibrous scaffolds on day 14. Dual labeling includes tetramethylrhodamine isothiocyanate-conjugated phalloidin (staining red F-actin) and 4′,6-diamidino-2-phenylindole, dilactate (staining blue nuclei). The staining showed the formation of an actin cytoskeleton in a 3D architecture for the cells cultured on the 3D scaffolds.

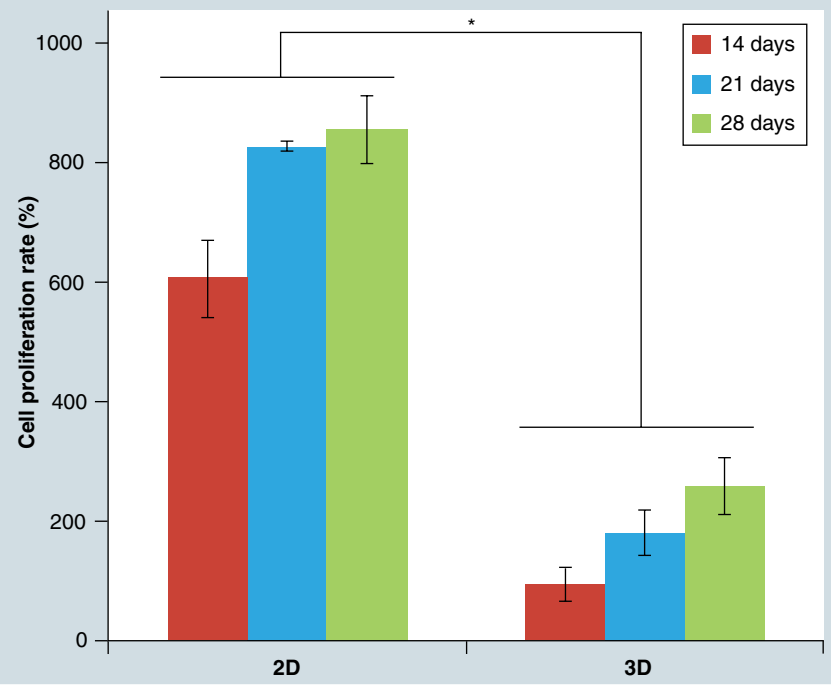

Figure 5. Cell proliferation rate of human mesenchymal stem cells differentiated in the osteogenic medium on 2D and 3D electrospun poly(L-lactic acid)/collagen type I nanofibrous scaffolds on days 14, 21 and 28. The cells on the 3D scaffolds had a significantly lower proliferation rate than those on the 2D scaffolds.
Significant difference of investigated groups is denoted as * ($p < 0.05$).
Error bars represent the standard deviation of three independent measurements.

geometry, and some of them started to form 3D shapes (Figure 3B). The F-actin staining on day 14 also showed the formation of an actin cytoskeleton in a 3D architecture for hMSCs cultured on 3D scaffolds (Figure 4).

Cell proliferation

The changes in the proliferation of differentiated hMSCs on both scaffolds during 14, 21 and 28 days of culture are demonstrated in Figure 5. The cell proliferation rate was calculated as the percent change from the original to the collected time point. With the same initial cell-seeding density of 10^4 cells/mg scaffold, the cells on the 2D and 3D scaffolds grew at different rates during the culture. The cells on 3D scaffolds had a lower rate than those on 2D scaffolds. However, while the cells on the 3D scaffolds continued to grow during 28 days of culture, the cells on the 2D scaffolds reached confluence and stopped proliferation after 21 days.

Osteoblastic gene expression

The expressions of osteoblastic genes including *ALP*, *OPN*, *OCN* and *WNT5A* of differentiated hMSCs on the 2D and 3D scaffolds after 14 and 21 days in culture are shown in Figure 6. On day 14, the cells differentiated on the 3D scaffolds had significantly higher expressions of all the osteoblastic genes. On day 21, the expression of *ALP* was still higher, but there was no considerable difference in the expressions of *OPN*, *OCN* and *WNT5A* of the cells on the 2D and 3D scaffolds.

Matrix mineralization

The formation of bone minerals on the 2D and 3D scaffolds at predetermined time points (14 and 28 days) was observed and identified by SEM-EDX as shown in Figures 7 & 8 & Supplementary Figures 2–5. On day 14, there were only a few minerals produced on the 2D surfaces (Figure 7A), but a lot of minerals were formed on the 3D scaffolds (Figure 7C & Supplementary Figure 2). Moreover, the bone minerals on the 3D scaffolds were significantly different from those on the 2D scaffolds. Looking at the EDX spectra of the minerals, it could be seen that the Ca and P peaks on the 3D scaffolds (Figure 7D) were clearly shown at high levels, whereas, those on the 2D scaffolds (Figure 7B) were very low. Although there is no scale on the y-axis of the EDX spectra, the levels of the Ca and P peaks can be compared to the C and O peaks. The Ca and P peaks in Figure 7D were much higher than those peaks in Figure 7B in comparison with the C and O peaks, respectively.

The morphologies of bone minerals were also different between the 2D and 3D scaffolds. The bone minerals looked like flakes on the 2D scaffolds, but bone nodules were produced on the 3D scaffolds. As such, after 14 days in culture, hMSCs differentiated on the 3D scaffolds secreted much more mature bone minerals than those on the 2D scaffolds.

On day 28, many bone nodules were produced on the 2D scaffolds (Figure 8A & B). Meanwhile, an extremely high density of bone minerals was formed on the outer and inner edge of the 3D scaffolds (Figures 8C–F & Supplementary Figures 4 & 5). Large bone aggregates were observed with a size of up to 50 µm on the 3D scaffolds (Figure 8E & Supplementary Figure 4B), whereas aggregates only up to 10 µm were observed on the 2D scaffolds (Figure 8A). Notably, it was solely observed on the 3D scaffolds where bone nodules were deposited along the nanofibers to form a mineralized matrix mimicking the native bone ECM (Figure 8C & F & Supplementary Figure 5A). The calculation of Ca:P ratios as well as statistical analysis ($p < 0.05$) also indicated a higher bone quality on the 3D scaffolds, with the ratio of 1.763 ± 0.056 for the 3D scaffolds, and

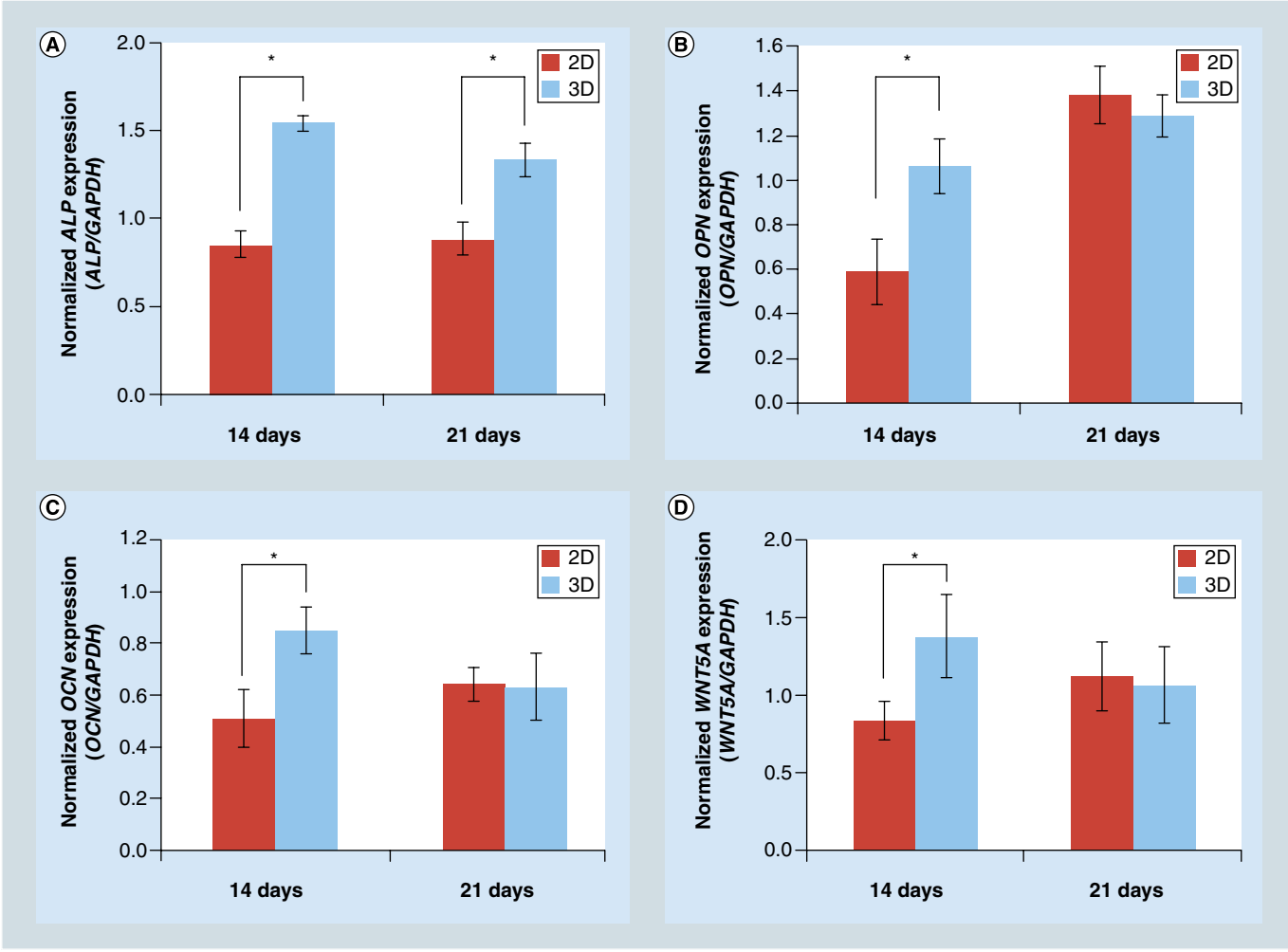

Figure 6. Normalized gene expression of human mesenchymal stem cells differentiated in the osteogenic medium on 2D and 3D electrospun poly(L-lactic acid)/collagen type I nanofibrous scaffolds on days 14 and 21. (A) *ALP*, **(B)** *OPN*, **(C)** *OCN* and **(D)** *WNT5A*. The osteogenic markers were significantly higher in 3D scaffolds up to 14 days and equated those of 2D scaffolds beyond 14 days (except for *ALP*).
Significant difference of investigated groups is denoted as *($p < 0.05$).
Error bars represent the standard deviation of three independent measurements.

1.402 ± 0.024 for the 2D scaffolds. In addition, there were some cells in a 3D shape on the 3D nanofibrous scaffolds (Figure 8D).

The quantification of calcium content produced by differentiated hMSCs on both scaffolds after 21 and 28 days cultured is shown in Figure 9A. Although Ca^{2+} and $H_2PO_4^-$ which present in the α-MEM can precipitate on the scaffolds to form hydroxyapatite, our experiment showed that during 28 days of the *in vitro* study, there was no calcium deposition on both 2D and 3D scaffolds incubated with the osteogenic medium (α-MEM supplemented with β-glycerophosphate, ascorbate-2-phosphate and dexamethasone, in the absence of the cells. As such, the calcium contents found in this study were purely derived from the differentiated cells. The amount of calcium secreted per cell on the 3D scaffolds was significantly higher than those on the 2D scaffolds ($p < 0.05$), approximately five-times. The 3D scaffolds also demonstrated a large amount of total calcium deposition as shown by a dense orange–red mass in Alizarin red S staining (Figure 9C) in comparision with lighter orange–red spots on the 2D scaffolds (Figure 9B). The formation and distribution of bone minerals within the 3D scaffolds are shown by micro-computed tomographic images (Figure 10). The bone minerals were distributed throughout the scaffolds quite evenly, with considerably higher density on day 28 (Figure 10C) compared with those on day 14 (Figure 10B).

Discussion

To guide cell behavior, it is important to design 3D scaffolds mimicking the structure of the native

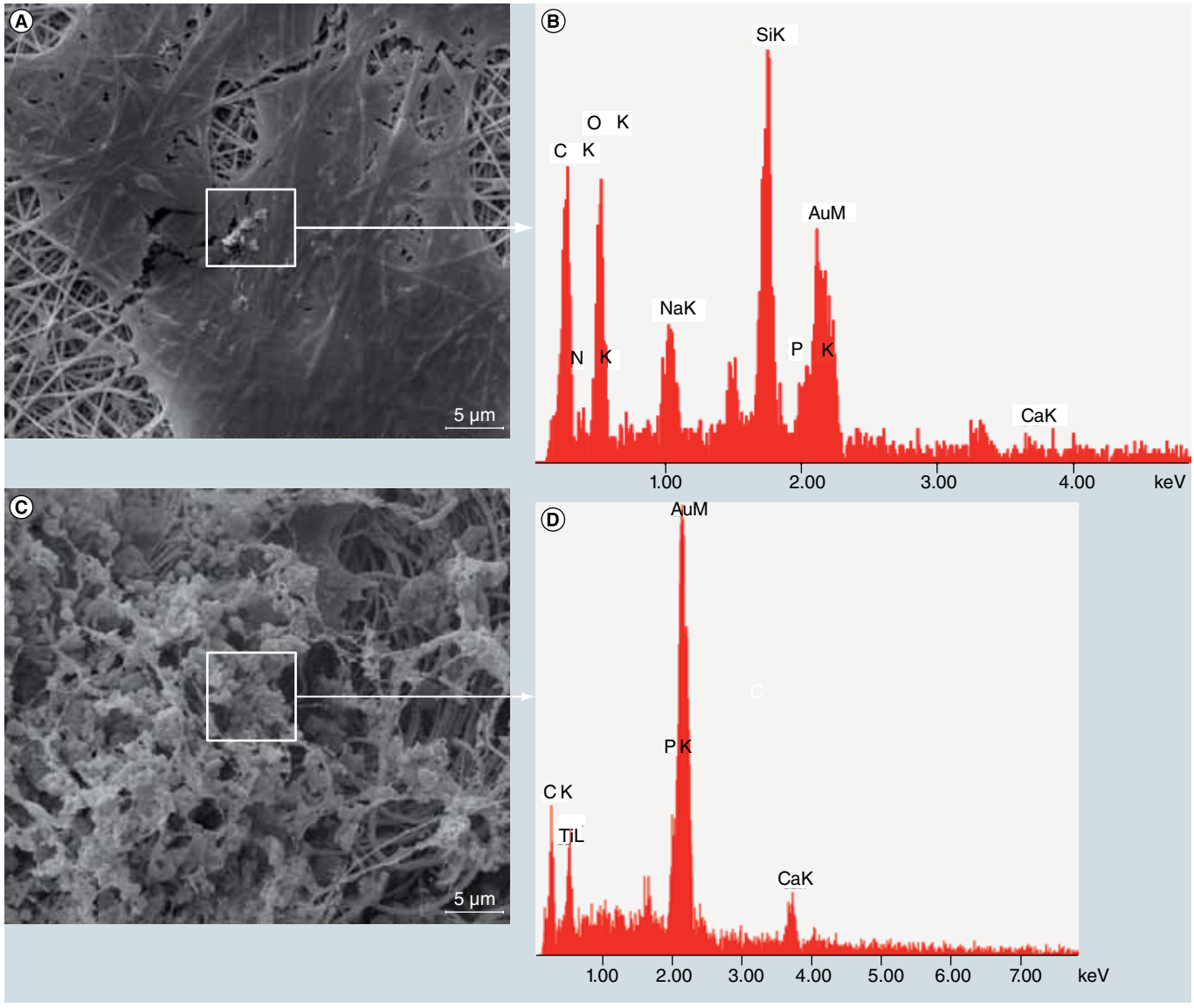

Figure 7. Scanning electron microscopic images and their energy dispersive x-ray spectra of poly(L-lactic acid)/collagen type I scaffolds. The scanning electron microscopy images at 5000× magnification of **(A)** 2D and **(C)** 3D electrospun poly(L-lactic acid)/collagen type I nanofibrous scaffolds cultured with human mesenchymal stem cells in the osteogenic medium on day 14, and **(B & D)** their respective energy dispersive x-ray spectra of the indicated minerals. There were only a few minerals produced on the 2D surfaces, but a lot of minerals were formed on the 3D scaffolds.

ECM. For a long time, electrospun nanofibers have been employed to mimic the nanostructure of collagen nanofibrils of the ECM. However, most of the electrospun nanofibrous structures used in previous studies have been 2D membranes with limited pore sizes, approximately 1–2 µm [24–26]. With these sizes, although 2D scaffolds have many layers of nanofibers deposited, the seeded cells cannot migrate deeply into the scaffolds to create a 3D structure of multilayered cells. Recently, we developed an electrospinning technique that is able to fabricate 3D nanofibrous assemblies with the pore size of approximately 50 µm, enough for supporting cell ingrowth and migration to create a 3D cell–matrix structure [20,21]. As such, the difference in pore size makes a difference in the dimensionality of cell–matrix structures (2D vs 3D). In this study, we demonstrated the advantages of this 3D scaffold over the conventional 2D electrospun nanofibrous scaffold in the osteogenic differentiation of hMSCs. In addition, the novelty of our 3D scaffold in comparison with other available 3D systems in enhancing the osteogenesis was emphasized.

Advantages of 3D scaffolds over 2D scaffolds

Although many studies have shown the advantages of 3D scaffolds over 2D scaffolds, it has been very difficult to conclude whether another

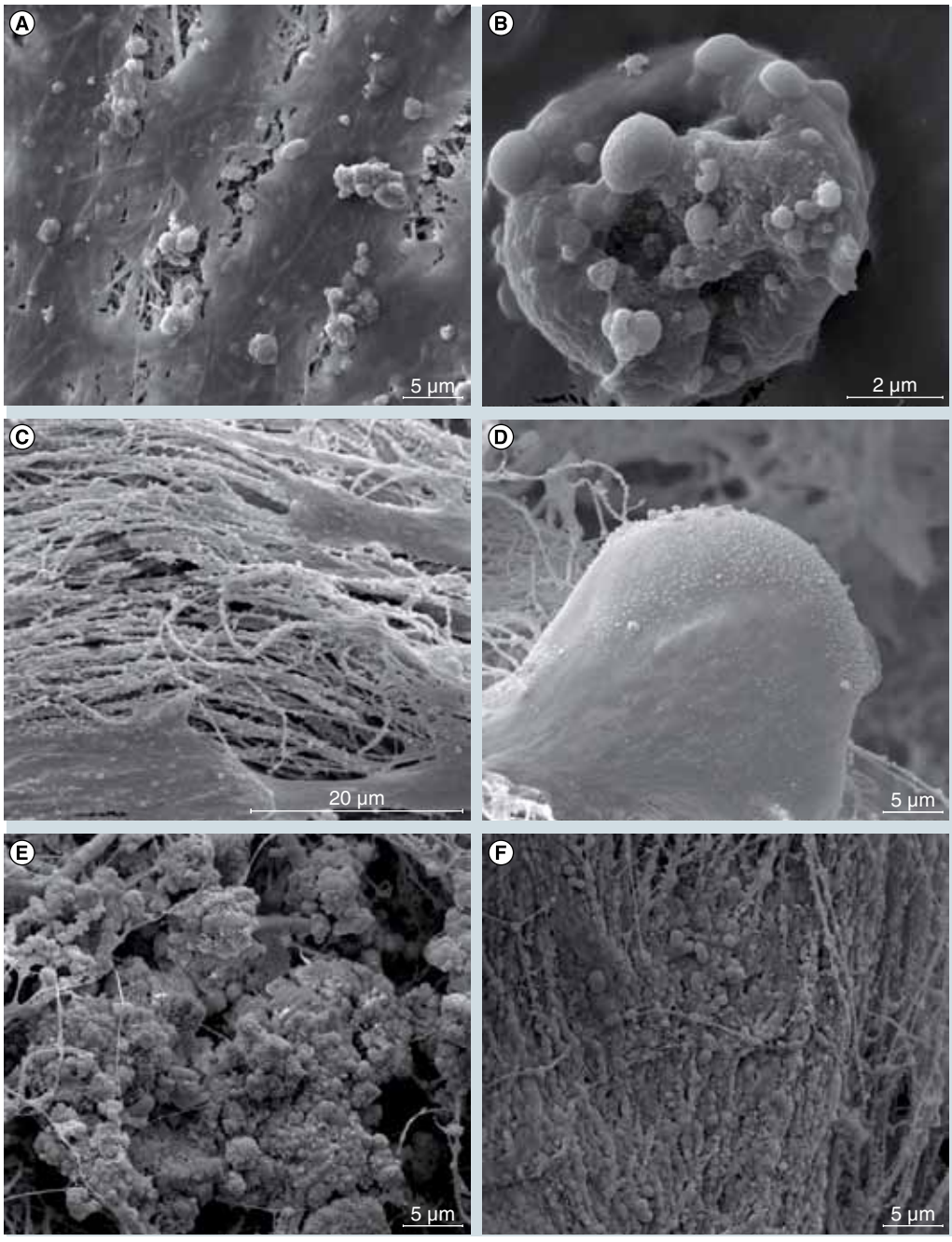

Figure 8. Scanning electron microscopic images of 2D and 3D electrospun poly(L-lactic acid)/collagen type I nanofibrous scaffolds cultured with human mesenchymal stem cells. The scanning electron microscopic images of **(A & B)** 2D, **(C & D)** the outer surface of 3D and **(E & F)** the center of 3D electrospun poly(L-lactic acid)/collagen type I nanofibrous scaffolds cultured with human mesenchymal stem cells in the osteogenic medium on day 28. **(C & F)** The deposition of bone minerals along the nanofibers at 5000× magnification. **(E)** The formation of large bone aggregates at 5000× magnification. **(D)** The presence of 3D-shaped cells at 5000× magnification.

dimension provided by 3D structures would help to increase cellular responses or not. Most of the studies have used TCP as a 2D surface to compare with 3D scaffolds [7–15,18,19,27]. It is obvious to see that there are two fundamental differences between TCP and 3D scaffolds: chemical natures and physical structures. Thus, it is not reliable to draw a conclusion on the role of 3D structures in this way. Some studies designed better systems where collagen sponges [16,17] and collagen gels [1] were compared to collagen-coated TCP in the protrusion and migration of endothelial cell, and the differentiation of ESCs into hepatocytes, respectively. However, the initial cell-seeding

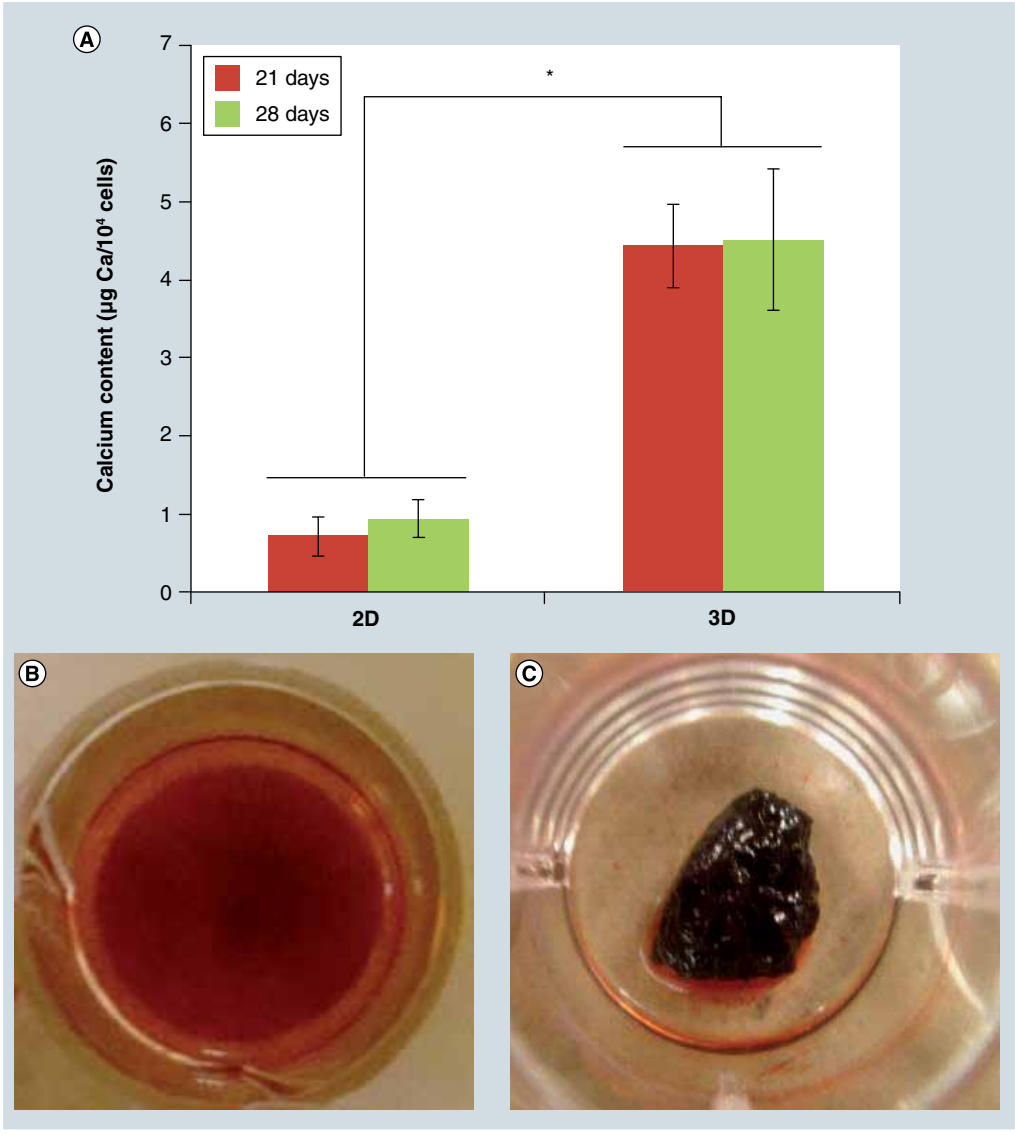

Figure 9. Calcium content produced by human mesenchymal stem cells on 2D and 3D scaffolds and Alizarin red S staining of the 2D and 3D scaffolds. (A) Calcium content produced by human mesenchymal stem cells differentiated in the osteogenic medium on 2D and 3D electrospun poly(L-lactic acid)/collagen type I nanofibrous scaffolds on days 21 and 28, and Alizarin red S staining of the **(B)** 2D and **(C)** 3D scaffolds on day 28. The amount of calcium secreted per cell on the 3D scaffolds was significantly higher than that on the 2D scaffolds. Significant difference of investigated groups is denoted as * ($p < 0.05$).
Each vertical error bar on the columns represents the standard deviation of three independent measurements.

density, which is important to the abilities of cellular proliferation and differentiation during cell culture, was randomly chosen in these studies with no criteria given for the 2D and 3D structures.

In our study, both 2D and 3D scaffolds were nanofibers made from PLLA/Col and fabricated by electrospinnning, with no statistically significant difference in fiber diameters between these scaffolds. They also possessed similar specific surface areas (data not shown). In addition, the cells were seeded on 2D and 3D scaffolds at the same density of 10^4 cells/mg scaffold. As such, the 2D and 3D scaffolds employed in this study appeared to be the same in chemical nature (PLLA/Col), size (nanofibers with similar diameters) and initial cell-seeding density. The role of dimensionality (2D vs 3D) in the osteogenic differentiation of hMSCs, therefore, would be demonstrated in a more conclusive way. However, owing to the difference in fabrication method, there were differences in morphology and mechanical property of these scaffolds. The nanofibers of the 2D scaffold, which were deposited on a flat and solid

Figure 10. Micro-computed tomographic images of the 3D electrospun poly(L-lactic acid)/collagen type I nanofibrous scaffold. (A) Micro-computed tomographic images of the original 3D electrospun poly(L-lactic acid)/collagen type I nanofibrous scaffold and the scaffold cultured with human mesenchymal stem cells in the osteogenic medium after **(B)** 14 and **(C)** 28 days. The bone minerals were distributed throughout the scaffolds quite evenly, with considerably higher density on day 28.

surface, were stiffer and appeared random and straight. Meanwhile, deposited on a liquid surface, the nanofibers of the 3D scaffold were softer and formed curved and coiled bundles. Matrix stiffness has been shown as one of the key factors that influence stem cell behaviors [28,29]. So, the difference in matrix stiffness of the 2D and 3D scaffolds may play a part in their various responses on the osteogenic differentiation of hMSCs.

While hMSCs on the 2D scaffolds were flattened on the surface (Figures 3A, 7A & 8A), there was an appearance of some 3D-shaped cells on the 3D scaffolds (Figures 3B & 8D). Although the proliferation rate of hMSCs on the 3D scaffolds was significantly lower than on the 2D scaffolds during 28 days of culture, the cells on the 3D scaffolds continued to grow throughout the study (Figure 5). Meanwhile, the cells on the 2D scaffolds seemed to reach confluence and stop their proliferation from the 21st day onwards. Some previous studies showed higher cell numbers on 3D scaffolds than on 2D scaffolds at all investigated time points [8–10]. However, the initial cell-seeding densities of these studies were not comparable, and TCP – a totally different object – was used as a 2D control. In other studies, it was indicated that while MSCs on 2D surfaces had a higher initial rate, they stopped their growth as confluence was reached; the cells in 3D scaffolds grew at a stable and lower rate, but lasted for a longer time and achieved a higher final cell number [11,12]. As such, these studies supported our observation. It could be said that if our *in vitro* study had been performed for a longer time, the cells in the 3D scaffolds would have reached a higher proliferation rate.

Despite the lower proliferation rate, the osteogenic functions of hMSCs on the 3D scaffolds were remarkably higher than on the 2D scaffolds as shown by the expression of osteoblastic genes (Figure 6) and the matrix mineralization (Figures 7–9). One possible reason for the lower proliferation rate of MSCs on the 3D scaffolds is that in the osteogenic medium, the MSCs were induced to differentiate into osteoblastic cells. In response to the medium, the 3D scaffolds accelerated signals/interactions/reactions towards the osteogenic differentiation pathway in comparison with the 2D scaffolds. It was well accepted that when stem cells underwent extensive differentiation, their proliferation could be reduced [30], and vice versa. Therefore, the proliferation rate of hMSCs on the 3D scaffolds was lower than the 2D scaffolds during the course of the study.

We tested the gene expression of various markers during the osteogenic differentiation, including ALP (an early marker, necessary for mineralization process by hydrolyzing organic phosphate to inorganic phosphate, which results in the precipitation of hydroxyapatite), OPN, OCN (middle and late markers, binding to hydroxyapatite and modulating the crystal growth) and WNT5A (a growth factor, strongly stimulating osteogenesis) [31,32]. The osteogenic markers were higher in 3D scaffolds up to 14 days and equated those of 2D scaffolds beyond 14 days (except for ALP). We chose days 14 and 21 to investigate the gene expression, as in the osteogenic condition, the expression of osteoblastic genes of hMSCs usually peak within this period. Looking at the expression of *ALP* (Figure 6A), it can be seen that there was a tendency towards a decreased expression of *ALP* from day 14 to 21 in the 3D scaffolds, but it did not significantly change in the 2D scaffolds. Normally, *ALP* increases in the early stage and then decreases when the culture becomes well mineralized [31]. Thus, it can be said that the ECM of hMSCs differentiated on the 3D

scaffolds became well mineralized earlier than those on the 2D surfaces. As such, the expression of the osteoblastic genes could help to explain the early formation and the impressive amount of bone nodules produced on the 3D scaffolds in comparison with the 2D scaffolds. Large bone aggregates, highly mineralized nanofibers and significantly increased calcium deposition were found on the 3D nanofibrous scaffolds.

From the results discussed, it can be concluded that the 3D PLLA/Col nanofibrous scaffolds increased and accelerated the osteogenic differentiation of hMSCs compared with the 2D scaffolds. There are some possible reasons to explain the role of 3D systems. In addition to closely mimicking tissue architecture *in vivo*, 3D environments provide another dimension for cell adhesion and external mechanical inputs. The enhancement in cell adhesion remarkably affects cell contraction, integrin ligation and related intracellular signals [33,34]. Besides, another dimension provided by 3D structures aided to enhance cell–matrix interactions and cell–cell communications [19]. These are important for regulating many cell signaling pathways to efficiently promote tissue development [35]. They may also lead to correct ECM organization and the increase of differentiation abilities [36,37].

The novelty of 3D electrospun nanofibrous scaffolds

In addition to claiming the advantages of 3D scaffolds over 2D scaffolds, our aim in this work was to indicate the novelty of the 3D electrospun PLLA/Col nanofibrous scaffolds in the osteogenic differentiation of hMSCs. Until now, most of the 3D biomaterials used for bone regeneration have been macro- or micro-sized structures, which can be fabricated by various methods such as thermally induced phase seperation, solvent casting, gas forming and rapid prototyping (including stereolithography, laser sintering, 3D printing and fused deposition modeling) [38–41]. However, mimicking the nanoscale structure of the native ECM is important for stimulating the healing and the regeneration of tissues and organs. In addition, with a large surface area-to-volume ratio, nanofibers provide more binding sites to cell membrane receptors and promote the adsorption of serum proteins [42,43], which may create a better niche to enhance cellular functions. Nanofibers are defined as fibers with diameters from 1 to 1000 nm. The significant support of nanofibrous structure in the osteogenic differentiation of hMSCs was indicated in our previous study [44]. Currently, modified thermally induced phase seperation and self assembly are two common techniques to fabricate 3D nanofibrous scaffolds for bone regeneration. Modified thermally induced phase seperation is a technique to fabricate nanofibrous foam materials. There are five basic steps in this technique: polymer dissolution, phase separation and gelation, solvent extraction from the gel with water, freezing, and freeze-drying under vacuum. The formation of the nanofibrous structure is postulated to be caused by spinodal liquid–liquid phase separation of the polymer solutions and consequential crystallization of the polymer-rich phase [45,46]. Self assembly is a bottom-up process in which small molecules spontaneously assemble into well-ordered nanofibers. The formation of this structure is induced by many interactions, including chiral dipole–dipole interactions, π–π stacking, hydrogen bonds, nonspecific van der Waals interactions, hydrophobic forces, electrostatic interactions and repulsive steric forces. Normally, the basic molecules to fabricate nanofibers using this technique are peptide amphiphiles [9,10,47–49]. Nevertheless, these techniques are not able to make long, continuous and uniform nanofibers, as well as being limited in material selection. These problems can be overcome by the electrospinning technique. This technique can fabricate a wide range of materials including synthetic, natural and blended polymers such as poly(lactic acid), poly(ε-caprolactone), poly(ethylene/vinyl acetate), polyurethane, poly(vinyl alcohol), PLGA, poly(ester urethane)urea, Col, gelatin, fibrinogen, chitosan, silk, gelatin/poly(ε-caprolactone), Col/poly(ester urethane)urea, among others [50]. Although the electrospining technique has been well explored for the fabrication of nanofibrous scaffolds in bone tissue engineering, these scaffolds have only been based on 2D meshes/membranes with limited pore sizes [44,51,52]. However, to efficiently treat large bone defects, it is necessary to develop truly 3D nanofibrous matrices. To the best of our knowledge, this is the first study where 3D electrospun nanofibrous scaffolds have been employed for the osteogenic differentiation of hMSCs.

PLLA and collagen with the ratio of 80:20 w/w were chosen to fabricate the nanofibrous materials in our study. Col has a rapid degradation rate and weak mechanical property [38], but it is important for initial cell adhesion and proliferation. The degradation of collagen can be found after 1 week of culture. Meanwhile, with a high mechanical property and a low degradation rate of up to 24 months [38], PLLA is very stable during the

in vitro study. Therefore, the structures of both scaffolds were well-maintained in the study.

Our study demonstrated impressive results for osteogenesis *in vitro* using the 3D electrospun PLLA/Col nanofibrous scaffolds. As early as day 14, a lot of bone minerals were deposited on nanofibers and many bone aggregates were produced on the 3D scaffolds (Figure 7C & Supplementary Figure 2). On day 28, bone nodules with a remarkably high density were formed on both the inside and the outside of the scaffolds (Figure 8C–F & Supplementary Figures 4 & 5). Very large bone aggregates were also found (Figure 8E & Supplementary Figure 4B). Notably, a vast number of the minerals were deposited on nanofibers which create an ECM matrix, mimicking the native bone ECM (Figure 8C & F & Supplementary Figure 5A). In addition, the Ca/P ratio of these minerals was 1.763 ± 0.056, similar to that ratio of hydroxyapatite of the native bone. In the native bone, collagen fibrils had a nanometer scale diameter range of 50–200 nm, and orderly deposited by nanohydroxyapatite mineral crystals. As such, differentiating hMSCs on the 3D electrospun nanofibrous scaffolds helped to create the ECM mimicking the nanostructure of the native bone and the bone mineral component. The almost uniform distribution of the bone minerals within the 3D structure was also clearly indicated by micro-computed tomographic images on days 14 and 28 (Figure 10). Although some other 3D nanofibrous scaffolds have been employed for the osteogenic differentiation of stem cells, there has been no study providing such obvious evidence of the bone-like ECM *in vitro*. They only presented the advantages of the scaffolds based on high expressions of osteoblastic genes and strong histological stainings (von Kossa and Alizarin red S) [9,10,45–47].

All of our results demonstrated a promising potential of using the 3D nanofibrous scaffolds to facilitate bone regeneration. These scaffolds can be utilized to implant directly to bone defects, or culture with hMSCs in the osteogenic medium for 14–28 days to create a bone ECM matrix before implantation. Using the bone-mimicking matrix produced on the 3D nanofibrous

Executive summary

Background

- Almost all tissue cells reside in a 3D environment, therefore, developing 3D scaffolds plays an important role in studying and regulating cellular characteristics.
- 3D scaffolds have been shown to affect cell morphology, proliferation and differentiation when compared with 2D scaffolds.
- However, it is still difficult to confirm whether those advantages are due to another dimension provided by the 3D structures, as there are too many differences in chemical natures, physical structures and initial cell-seeding densities between the 2D and 3D structures.

Materials & methods

- A comparative study was set up to identify the role of 3D nanofibrous scaffolds fabricated by a modified electrospinning technique using a dynamic liquid support system in the osteogenic differentiation of human mesenchymal stem cells (hMSCs) during 28 days of culture. 2D nanofibrous scaffolds fabricated by the conventional electrospinning were used as controls.
- Both scaffolds were made from poly(L-lactic acid)/collagen type I (PLLA/Col) with the same initial cell-seeding density of 10^4 cells/mg scaffold.
- Analysis methods: scanning electron microscopy, actin cytoskeleton staining, cell proliferation by the MTS assay, osteoblastic gene expression (*ALP*, *OPN*, *OCN* and *WNT5A*), calcium content, Alizarin red S staining and micro-computed tomography.

Results

- There was no significant difference in the fibrous diameters of the 2D and 3D nanofibrous scaffolds.
- Some of the cells started to form 3D shapes on the 3D scaffolds.
- The cells on the 3D scaffolds had a lower proliferation rate than those on the 2D scaffolds, but they demonstrated a continuous growth over 28 days.
- On day 14, the cells differentiated on the 3D scaffolds had significantly higher expressions of all the osteoblastic genes than those on the 2D scaffolds.
- The 3D scaffolds showed greater amounts and better quality of bone minerals compared with the 2D scaffolds.
- The 3D electrospun nanofibrous scaffolds indicated a dense deposition of bone minerals aligned along nanofibers, the formation of large bone aggregates and the even distribution of the minerals within the 3D structures.

Discussion

- The role of dimensionality (2D vs 3D) in the osteogenic differentiation of hMSCs was demonstrated in our study in a more conclusive way.
- The 3D PLLA/Col nanofibrous scaffolds increased and accelerated the osteogenic differentiation of hMSCs compared with the 2D scaffolds.
- To the best of our knowledge, this is the first study where 3D electrospun nanofibrous scaffolds have been employed for the osteogenic differentiation of hMSCs.
- Our study showed impressive results of osteogenesis *in vitro* using 3D electrospun PLLA/Col nanofibrous scaffolds in comparison with other available scaffolds.

scaffolds could be a novel approach to induce an accelerated bone healing.

Conclusion

The 3D PLLA/Col nanofibrous scaffolds fabricated by the electrospinning technique supported by a dynamic liquid system showed significant advantages over the conventional 2D electrospun PLLA/Col nanofibrous scaffolds in the ostegenic differentiation of hMSCs. The cells cultured on the 3D scaffolds had significantly higher expressions of osteoblastic genes (*ALP*, *OPN*, *OCN* and *WNT5A*) as well as greater amounts and better quality of bone minerals. Some cells in 3D shapes were found on the 3D scaffolds. As such, the 3D physical structure played an important role in facilitating the osteogenic differentiation of hMSCs. In addition, with the dense deposition of bone minerals aligned along nanofibers, the formation of large bone aggregates and the even distribution of the minerals within the 3D structures, the 3D electrospun PLLA/Col nanofibrous scaffold deserves to be considered as a promising scaffold for bone regeneration.

Acknowledgements

The authors give many thanks to TW Eong for valuable discussions and VT Nghia at Singapore Synchrotron Light Source for helping us perform micro-computed tomography.

Financial & competing interests disclosure

The authors would like to thank National Medical Research Council (NMRC/1151/2008), Singapore, for financial support. The authors have no other relevant affiliations or financial involvement with any organization or entity with a financial interest in or financial conflict with the subject matter or materials discussed in the manuscript apart from those disclosed.

No writing assistance was utilized in the production of this manuscript.

Ethical conduct of research

The authors state that they have obtained appropriate institutional review board approval or have followed the principles outlined in the Declaration of Helsinki for all human or animal experimental investigations. In addition, for investigations involving human subjects, informed consent has been obtained from the participants involved.

References

Papers of special note have been highlighted as:
▪ of interest
▪▪ of considerable interest

1 Martins GG, Kolega J. Endothelial cell protrusion and migration in three-dimensional collagen matrices. *Cell Motil. Cytoskeleton* 63(2), 101–115 (2006).

2 Lee J, Cuddihy MJ, Kotov NA. Three-dimensional cell culture matrices: state of the art. *Tissue Eng. Part B Rev.* 14(1), 61–86 (2008).

3 Zhang S, Gelain F, Zhao X. Designer self-assembling peptide nanofiber scaffolds for 3D tissue cell cultures. *Semin. Cancer Biol.* 15(5), 413–420 (2005).

4 Albrecht DR, Underhill GH, Wassermann TB, Sah RL, Bhatia SN. Probing the role of multicellular organization in three-dimensional microenvironments. *Nat. Methods* 3(5), 369–375 (2006).

5 Lee GY, Kenny PA, Lee EH, Bissell MJ. Three-dimensional culture models of normal and malignant breast epithelial cells. *Nat. Methods* 4(4), 359–365 (2007).

6 Griffith LG, Swartz MA. Capturing complex 3D tissue physiology *in vitro*. *Nat. Rev. Mol. Cell. Biol.* 7(3), 211–224 (2006).

▪▪ **Highlights the importance of a 3D environment.**

7 Hwang NS, Kim MS, Sampattavanich S, Baek JH, Zhang Z, Elisseeff J. Effects of three-dimensional culture and growth factors on the chondrogenic differentiation of murine embryonic stem cells. *Stem Cells* 24(2), 284–291 (2006).

8 Liu H, Collins SF, Suggs LJ. Three-dimensional culture for expansion and differentiation of mouse embryonic stem cells. *Biomaterials* 27(36), 6004–6014 (2006).

9 Hosseinkhani H, Hosseinkhani M, Tian F, Kobayashi H, Tabata Y. Osteogenic differentiation of mesenchymal stem cells in self-assembled peptide-amphiphile nanofibers. *Biomaterials* 27(22), 4079–4086 (2006).

10 Hosseinkhani H, Hosseinkhani M, Kobayashi H. Proliferation and differentiation of mesenchymal stem cells using self-assembled peptide amphiphile nanofibers. *Biomed. Mater.* 1(1), 8–15 (2006).

11 Xie Y, Yang ST, Kniss DA. Three-dimensional cell-scaffold constructs promote efficient gene transfection: implications for cell-based gene therapy. *Tissue Eng.* 7(5), 585–598 (2001).

12 Cao Y, Li D, Shang C, Yang ST, Wang J, Wang X. Three-dimensional culture of human mesenchymal stem cells in a polyethylene terephthalate matrix. *Biomed. Mater.* 5(6), 065013 (2010).

13 Li J, Tao R, Wu W *et al.* 3D PLGA scaffolds improve differentiation and function of bone marrow mesenchymal stem cell-derived hepatocytes. *Stem Cells Dev.* 19(9), 1427–1436 (2010).

14 Li Y, Kniss DA, Lasky LC, Yang ST. Culturing and differentiation of murine embryonic stem cells in a three-dimensional fibrous matrix. *Cytotechnology* 41(1), 23–35 (2003).

15 Levenberg S, Huang NF, Lavik E, Rogers AB, Itskovitz-Eldor J, Langer R. Differentiation of human embryonic stem cells on three-dimensional polymer scaffolds. *Proc. Natl Acad. Sci. USA* 100(22), 12741–12746 (2003).

▪ **Demonstrated the enhanced hepatocyte differentiation of stem cells using 3D sponges.**

16 Imamura T, Cui L, Teng R *et al.* Embryonic stem cell-derived embryoid bodies in three-dimensional culture system form hepatocyte-like cells *in vitro* and *in vivo*. *Tissue Eng.* 10(11–12), 1716–1724 (2004).

17 Baharvand H, Hashemi SM, Kazemi Ashtiani S, Farrokhi A. Differentiation of human embryonic stem cells into hepatocytes in 2D and 3D culture systems *in vitro*. *Int. J. Dev. Biol.* 50(7), 645–652 (2006).

18 Garreta E, Genové E, Borrós S, Semino CE. Osteogenic differentiation of mouse embryonic stem cells and mouse embryonic fibroblasts in a three-dimensional self-assembling peptide scaffold. *Tissue Eng.* 12(8), 2215–2227 (2006).

19 Tian XF, Heng BC, Ge Z *et al.* Comparison of osteogenesis of human embryonic stem cells within 2D and 3D culture systems. *Scand. J. Clin. Lab. Invest.* 68(1), 58–67 (2008).

20 Teo W, Gopal R, Ramaseshan R, Fujihara K, Ramakrishna S. A dynamic liquid support system for continuous electrospun yarn fabrication. *Polymer* 48, 3400–3405 (2007).

21 Teo W, Liao S, Chan C, Ramakrishna S. Remodeling of three-dimensional hierarchically organized nanofibrous assemblies. *Curr. Nanoscience* 4(4), 361–361 (2008).

▪ **Highlights a technique to fabricate 3D electrospun nanofibrous scaffolds.**

22 Chastain SR, Kundu AK, Dhar S, Calvert JW, Putnam AJ. Adhesion of mesenchymal stem cells to polymer scaffolds occurs via distinct ECM ligands and controls their osteogenic differentiation. *J. Biomed. Mater. Res. A* 78(1), 73–85 (2006).

23 Shih YRV, Chen CN, Tsai SW, Wang YJ, Lee OK. Growth of mesenchymal stem cells on electrospun type I collagen nanofibers. *Stem Cells* 24(11), 2391–2397 (2006).

24 Li C, Vepari C, Jin HJ, Kim HJ, Kaplan DL. Electrospun silk BMP-2 scaffolds for bone tissue engineering. *Biomaterials* 27(16), 3115–3124 (2006).

25 Ma K, Chan CK, Liao S, Hwang WYK, Feng Q, Ramakrishna S. Electrospun nanofiber scaffolds for rapid and rich capture of bone marrow-derived hematopoietic stem cells. *Biomaterials* 29(13), 2096–2103 (2008).

26 Ngiam M, Liao S, Patil AJ, Cheng Z, Chan CK, Ramakrishna S. The fabrication of nano-hydroxyapatite on PLGA and PLGA/collagen nanofibrous composite scaffolds and their effects in osteoblastic behavior for bone tissue engineering. *Bone* 45(1), 4–16 (2009).

27 Ishaug SL, Crane GM, Miller MJ, Yasko AW, Yaszemski MJ, Mikos AG. Bone formation by three-dimensional stromal osteoblast culture in biodegradable polymer scaffolds. *J. Biomed. Mater. Res.* 36(1), 17–28 (1997).

28 Discher DE, Janmey P, Wang YL. Tissue cells feel and respond to the stiffness of their substrate. *Science* 310(5751), 1139–1143 (2005).

29 Guilak F, Cohen DM, Estes BT, Gimble JM, Liedtke W, Chen CS. Control of stem cell fate by physical interactions with the extracellular matrix. *Cell Stem Cell* 5(1), 17–26 (2009).

30 Pittenger MF, Mackay AM, Beck SC *et al.* Multilineage potential of adult human mesenchymal stem cells. *Science* 284(5411), 143–147 (1999).

31 Lian JB, Stein GS. Concepts of osteoblast growth and differentiation: basis for modulation of bone cell development and tissue formation. *Crit. Rev. Oral. Biol. Med.* 3(3), 269–305 (1992).

32 Santos A, Bakker AD, De Blieck-Hogervorst JMA, Klein-Nulend J. WNT5A induces osteogenic differentiation of human adipose stem cells via rho-associated kinase ROCK. *Cytotherapy* 12(7), 924–932 (2010).

33 Knight B, Laukaitis C, Akhtar N, Hotchin NA, Edlund M, Horwitz AR. Visualizing muscle cell migration *in situ*. *Curr. Biol.* 10(10), 576–585 (2000).

34 Roskelley CD, Desprez PY, Bissell MJ. Extracellular matrix-dependent tissue-specific gene expression in mammary epithelial cells requires both physical and biochemical signal transduction. *Proc. Natl Acad. Sci. USA* 91(26), 12378–12382 (1994).

35 Geiger B, Bershadsky A, Pankov R, Yamada KM. Transmembrane crosstalk between the extracellular matrix – cytoskeleton crosstalk. *Nat. Rev. Mol. Cell. Biol.* 2(11), 793–805 (2001).

36 Kale S, Biermann S, Edwards C, Tarnowski C, Morris M, Long MW. Three-dimensional cellular development is essential for *ex vivo* formation of human bone. *Nat. Biotechnol.* 18(9), 954–958 (2000).

37 Ferrera D, Poggi S, Biassoni C *et al.* Three-dimensional cultures of normal human osteoblasts: proliferation and differentiation potential *in vitro* and upon ectopic implantation in nude mice. *Bone* 30(5), 718–725 (2002).

38 Liao S, Chan CK, Ramakrishna S. Stem cells and biomimetic materials strategies for tissue engineering. *Mater. Sci. Eng. C* 28(8), 1189–1202 (2008).

39 Stevens B, Yang Y, Mohandas A, Stucker B, Nguyen K. A review of materials, fabrication methods, and strategies used to enhance bone regeneration in engineered bone tissues. *J. Biomed. Mater. Res. B Appl. Biomater.* 85(2), 573–582 (2008).

40 Wiria FE, Chua CK, Leong KF, Quah ZY, Chandrasekaran M, Lee MW. Improved biocomposite development of poly(vinyl alcohol) and hydroxyapatite for tissue engineering scaffold fabrication using selective laser sintering. *J. Mater. Sci. Mater. Med.* 19(3), 989–996 (2008).

41 Simpson RL, Wiria FE, Amis AA *et al.* Development of a 95/5 poly(L-lactide-*co*-glycolide)/hydroxylapatite and β-tricalcium phosphate scaffold as bone replacement material via selective laser sintering. *J. Biomed. Mater. Res. B Appl. Biomater.* 84B(1), 17–25 (2008).

42 Stevens MM, George JH. Exploring and engineering the cell surface interface. *Science* 310(5751), 1135–1138 (2005).

▪▪ **Indicates the importance of nanofibrous structure to cellular behaviors.**

43 Woo KM, Chen VJ, Ma PX. Nano-fibrous scaffolding architecture selectively enhances protein adsorption contributing to cell attachment. *J. Biomed. Mater. Res. A* 67(2), 531–537 (2003).

44 Nguyen LT, Liao S, Ramakrishna S, Chan CK. The role of nanofibrous structure in osteogenic differentiation of human mesenchymal stem cells with serial passage. *Nanomedicine (Lond.)* 6(6), 961–974 (2011).

45 Smith LA, Liu X, Hu J, Ma PX. The influence of three-dimensional nanofibrous scaffolds on the osteogenic differentiation of embryonic stem cells. *Biomaterials* 30(13), 2516–2522 (2009).

46 Smith LA, Liu X, Hu J, Ma PX. The enhancement of human embryonic stem cell osteogenic differentiation with nano-fibrous scaffolding. *Biomaterials* 31(21), 5526–5535 (2010).

47 Galler KM, Cavender A, Yuwono V *et al.* Self-assembling peptide amphiphile nanofibers as a scaffold for dental stem cells. *Tissue Eng. Part A* 14(12), 2051–2058 (2008).

48 Hosseinkhani H, Hosseinkhani M, Khademhosseini A, Kobayashi H. Bone regeneration through controlled release of bone morphogenetic protein-2 from 3-D tissue engineered nano-scaffold. *J. Control Release* 117(3), 380–386 (2007).

49 Hosseinkhani H, Hosseinkhani M, Tian F, Kobayashi H, Tabata Y. Ectopic bone formation in collagen sponge self-assembled peptide-amphiphile nanofibers hybrid scaffold in a perfusion culture bioreactor. *Biomaterials* 27(29), 5089–5098 (2006).

50 Chew S, Wen Y, Dzenis Y, Leong K. The role of electrospinning in the emerging field of nanomedicine. *Curr. Pharm. Des.* 12(36), 4751–4770 (2006).

51 Seyedjafari E, Soleimani M, Ghaemi N, Shabani I. Nanohydroxyapatite-coated electrospun poly(L-lactide) nanofibers enhance osteogenic differentiation of stem cells and induce ectopic bone formation. *Biomacromolecules* 11(11), 3118–3125 (2010).

52 Yang X, Yang F, Walboomers XF, Bian Z, Fan M, Jansen JA. The performance of dental pulp stem cells on nanofibrous PCL/gelatin/nHA scaffolds. *J. Biomed. Mater. Res. A* 93(1), 247–257 (2010).